EFFECT OF MUD CAKE AND TEMPERATURE ON WELLBORE COLLAPSE INITIATION PRESSURE USING DIFFERENT FAILURE CRITERIA

A Thesis

by

SHOLA DANIEL BABALOLA

Submitted to the Office of Graduate and Professional Studies of
Texas A&M University
in partial fulfillment of the requirements for the degree of

MASTER OF SCIENCE

Chair of Committee,	Jerome Schubert
Committee Members,	Sam Noynaert
	Fred Chester
Head of Department,	Daniel Hill

December 2015

Major Subject: Petroleum Engineering

ABSTRACT

Accurate wellbore collapse initiation pressure is necessary for a robust wellbore bridging study. When drilling overbalance through a porous and permeable formation, there is flow of wellbore fluid into the formation, leaving behind a solid mud cake on the formation. Formation strengthening by drilling fluids has been discussed extensively in the literature. This work attempts to study the coupled effect of mud cake and temperature on the collapse initiation pressure.

Sensitivity analysis using unequal horizontal stresses showed that the effect of mud cake on collapse initiation pressure is not affected by the mud cake compressibility but depends on mud cake thickness, rock unconfined compressive strength, stress level/magnitude and wellbore size. The presence of a mud cake reduces the collapse initiation pressure, making the formation more resistant to collapse. This effect increases as the mud cake thickness, unconfined compressive strength and stress level increase. A decrease in wellbore size also increases the effect of filter cake on collapse initiation pressure.

Generally, wellbore heating weakens the formation while cooling strengthens the formation. The presence of a mud cake acts similarly to cooling the wellbore. Coupling the effect of mud cake and temperature showed that the presence of mud cake increases the effect of both wellbore heating and cooling.

DEDICATION

I would like to dedicate this thesis to my mum. She has been a constant source of blessing and motivation to me.

ACKNOWLEDGEMENTS

I would like to express my appreciation to Dr. Jerome Schubert for accepting me into his group and giving me the chance to work on this project. Thanks to Dr. Sam Noynaert and Dr. Fred Chester for being part my advisory committee; your support and time is appreciated. Thanks to BORA for funding this project.

Thanks to Femi Oyedokun, for his support throughout this project. I would also like to say thank you to all occupants of Room 1007 between 2013 and 2015, it was nice sharing the office with you.

Finally, a big thank you to my family for their support throughout the duration of my Master's program.

NOMENCLATURE

c	Compressibility Exponent
E	Young's Modulus, psi
P_{mc}	Mud Cake Pressure, psi
P_w	Wellbore Pressure, psi
P_0	Pore Pressure, psi
r_{mc}	Wellbore Radius to Mud Cake Interface, in
r_w	Wellbore Radius to Formation Wall, in
S_{Hmax}	Maximum Horizontal Stress, psi
S_{hmin}	Minimum Horizontal Stress, psi
S_0	Cohesion, psi
S_v	Vertical Stress, psi
T_{mc}	Mud Cake Thickness, mm
UCS	Unconfined Compressive Strength, psi
v	Poisson's Ratio
ΔT	Temperature Difference between Wellbore Fluid and Formation, ^0C
α	Coefficient of Linear Thermal Expansion, $/^0C$
Φ	Angle of Internal Friction, degree
θ	Angle Around Wellbore Measured from S_{Hmax}
$\emptyset_{mc}$	Mud Cake Porosity at P_{mc}
$\emptyset_{mc0}$	Reference Mud Cake Porosity

μ	Coefficient of Internal Friction
τ	Shear Stress, psi
σ_h	Horizontal Stress, psi
σ_1	Maximum Principal Stress, psi
σ_2	Intermediate Principal Stress, psi
σ_3	Minimum Principal Stress, psi
σ'_n	Effective Normal Stress, psi
σ'_{rr}	Effective Radial Stress, psi
σ'_{zz}	Effective Axial Stress along Wellbore Axis, psi
$\sigma'_{\theta\theta}$	Effective Hoop Stress, psi
$\sigma_{rr}^{\Delta T}$	Thermally Induced Radial Stress, psi
$\sigma_{\theta\theta}^{\Delta T}$	Thermally Induced Hoop Stress, psi
$\sigma_{zz}^{\Delta T}$	Thermally Induced Axial Stress, psi

TABLE OF CONTENTS

Page

LIST OF FIGURES

LIST OF TABLES

CHAPTER I

INTRODUCTION

1.1 Overview

Accidents have occurred in the oil industry due to uncontrolled flow of formation fluids. A kick is said to be taken when there is an unscheduled flow of formation fluid into the wellbore because wellbore pressure is lower than formation pore pressure. A blowout, which is an uncontrolled and continuous flow of formation fluids out of the well when a kick cannot be brought under control, can lead to great loss in pollution, investment and lives. It is a very challenging problem caused by human error, equipment failure or a combination of both. A blowout can be surface, subsurface (at mud line) or underground blowout.

After a blowout has occurred, control over the well needs to be regained so as to mitigate the impact of the blowout. Techniques that can be used to regain control of the well after blowout include capping, closing of blowout preventer, pumping cement slurry, pumping mud, depletion or water breakthrough in shallow gas blowout, crew intervention, drilling of relief well (Figure 1.1) and bridging (Skalle et al. 1999, Smith 2012). Most of these kill mechanisms are well understood but bridging.

At the point when a kick is taken, formation pressure is greater than the wellbore pressure thereby leading to flow from formation into the wellbore. As formation fluids flow into the wellbore, so does the hydrostatic pressure in the wellbore drop. As wellbore pressure decreases, some open interval of the wellbore may experience wellbore

instability. If the quantity of caved rock is sufficient enough, it will choke flow and eventually kill the blowout (Figure 1.2). This kill mechanism is termed bridging (Adams and Kuhlman 1991, Danenberger 1993, Jourine et al. 2004, Nesheli and Schubert 2006, Wilson 2012).

As part of measures to ensure a safer environment, the Bureau of Safety and Environmental Enforcement requires all new well permits to provide a scenario for worst case hydrocarbon discharge for the proposed wells during a potential blowout. As part of this regulation, the chances for the well to bridge over are also to be considered (BOEM NTL No. 2010-N06).

A lot of work in the area of bridging has just been able to describe bridging qualitatively. Wilson (2012) and Wilson et al. (2013) proposed four analyses for wellbore bridging investigation. The four analyses are kick-development, assessment of borehole collapse, caving volume and transport analysis, and caving bridging. This work will focus on the assessment of borehole collapse analyses area. For accurate wellbore bridging study, accurate determination of collapse initiation pressure is important. While drilling overbalance, there is flow of wellbore fluid into the formation, leaving behind a solid filter cake on the formation. This work, which is a part of a wellbore bridging project, will study the effect of filter cake and temperature on collapse initiation pressure and recommend if this is to be considered when determining collapse initiation pressure for a wellbore bridging investigation.

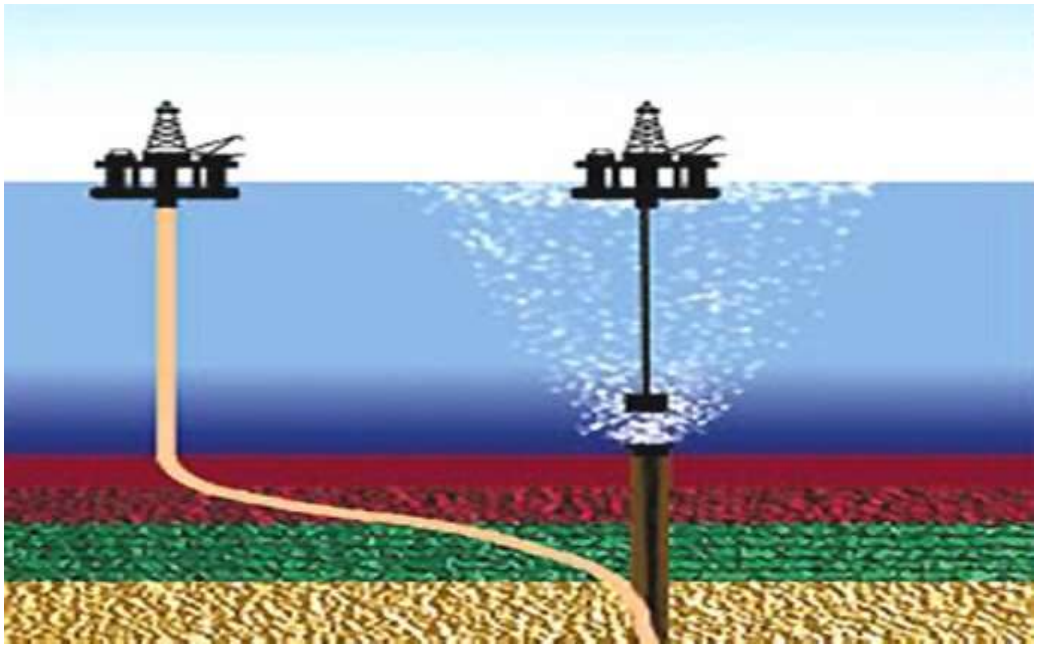

Figure 1.1: Relief well (Grøttheim 2005).

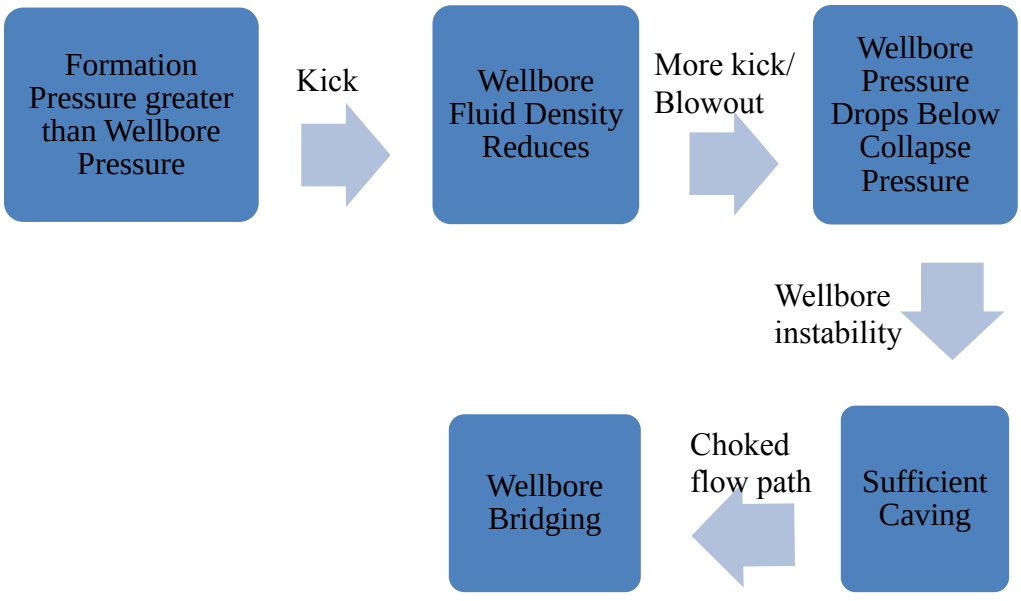

Figure 1.2: Schematic showing how wellbore bridging can occur.

CHAPTER II

LITERATURE REVIEW

2.1 Wellbore Bridging

Wellbore bridging is a well-known method for stopping many shallow gas blowout especially on land and shallow water depths. The ability of over-pressured shallow sand reservoirs, especially those in deep water, to be self-killing (bridge) have been questioned by recent evidence from deep-water shallow water flows. These well do not bridge even though they carry large volumes of entrained solids (Wilson 2012). Wilson (2012) and Wilson et al. (2013) suggested that bridging leading to self-killing of a blowout can only occur in few situations in deep-water, which is contrary to data available from shallow water Gulf of Mexico shelf wells. Bridging depends largely on the formation properties with little or no control by human.

Wellbore bridging is inhibited by cased hole, low flow rates, deep water environments with sea backpressure, surface obstructions preventing open flow and stable competent formations, and supported by shallow casing strings, formation instability under drawdown situations, gas blowout fluids, high flow rates and low or shallow water depths (Adams and Kuhlman 1991).

Between 1971 and 1991, 87 blowouts (84 oil and gas) occurred in the Outer Continental Shelf (OCS) during drilling operations, 58 of these blowouts occurred in depth less than 5000ft. 62 of those 87 blowouts were killed through bridging (Figure 2.1) and the blowouts in wells that bridged lasted short duration (55 lasted less than one week)

(Danenberger 1993). Similarly, Skalle et al. (1999) analyzed 1120 blowout events that occurred between 1960 and 1996 in the Gulf Coast and adjoining states. They found that 39.6% of blowouts in the OCS (Figure 2.2) and 19 % in Texas (Figure 2.3) were controlled through bridging.

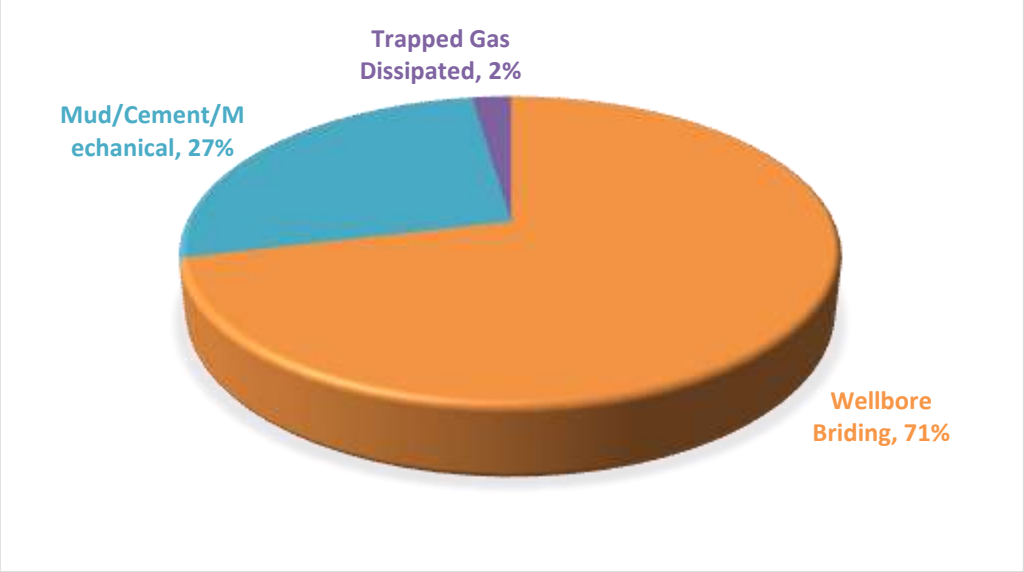

Figure 2.1: Kill technique used to control blowouts in OCS from 1971-1991 (Danenberger 1993).

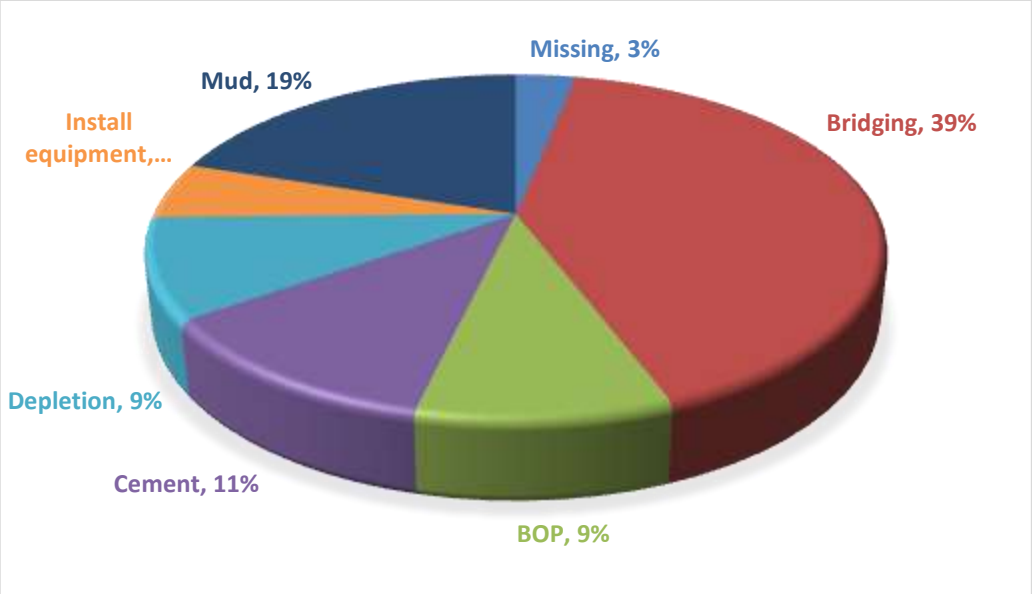

Figure 2.2: Kill technique used to control blowouts in OCS from 1971-1999 (Skalle et al. 1999).

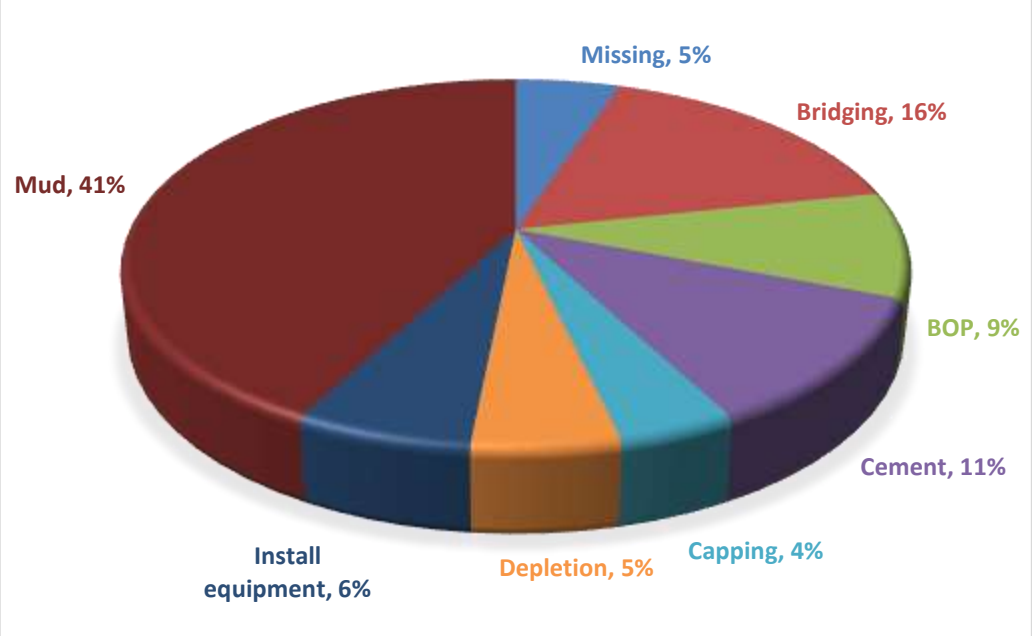

Figure 2.3: Kill technique used to control blowouts in Texas from 1971-1999 (Skalle et al. 1999).

Nesheli and Schubert (2006) used wellbore breakout to predict bridging tendency in deep-water wells. They conducted their simulations for shale intervals and concluded the depth at which wellbore collapse occurs depends on both depth of water and the direction of maximum stress. Their model predicted wellbore failure. However, they did not quantify caving volume, neither did they discuss caving transport.

Wilson (2012) and Wilson et al. (2013) presented an analysis approach to assess borehole stability and the likelihood of bridging. These works suggested that, before the occurrence of bridging can be accurately predicted, four analyses need to be carried out. First, kick-development analysis, which helps to develop pressure and in-flow velocity profile of the well after the kick. Second, assessment of borehole collapse, which predicts formation failure from drawdown deduced from wellbore pressure profile. Third, caving volume and transport analysis, which helps to quantify the failed rocks and determine if they will be transported as entrained solids. And fourth, caving bridging analysis, which helps to assess if bridging can occur from the concentration of caving in various locations in the wellbore. Their analyses suggested that, for deep-water reservoirs, bridging can be relied on as a means of shutting a flowing well if the kick was as a result of loss of riser margin when the drill pipe is in the open-hole interval of the wellbore. They also suggested that bridging can only be relied on if it occurred while the kick is still developing (before hydrocarbon gets to the wellhead). After the kick has developed, caving will be transported without bridging.

This work will focus on the borehole collapse/instability area of wellbore bridging study, showing how mud cake and temperature affect it.

2.2 Wellbore Stability

2.2.1 Introduction

Wellbore failure is necessary for bridging to occur. Typically, failure is not desired during drilling, but in this case has a positive impact because of its capability to arrest a kick or blowout. A stable wellbore is always desired during drilling and production. Wellbore instability costs the oil and gas industry over 6 billion USD every year (Kang et al. 2009), and is even more critical as the oil and gas venture into more difficult formations like those encountered in mountainous regions, High Pressure High Temperature (HPHT) wells, shale gas, gas hydrates and extended reach wells. Most wellbore failure during drilling operations occur in shale intervals; these rocks are very abundant in the sedimentary basins where we find oil and gas.

Before drilling, the formation is in a state of equilibrium and three principal compressive stresses exist within it. In a normal fault environment, the overburden stress (S_v) is the maximum principal stress (σ_1), the minimum horizontal stress (S_{hmin}) is the minimum principal stress (σ_3) and the maximum horizontal stress (S_{Hmax}) is the intermediate principal stress (σ_2). After a hole has been created, drilling fluid replaces drilled rock. This leads to redistribution of stresses around the borehole because the support offered by drilled rocks is replaced by pressure of the drilling fluid (pressure of drilling fluid may be from the hydrostatic pressure, pump pressure, surge, swab or back pressure applied from surface). The redistributed stresses are the hoop or tangential stress, which act along the circumference of the wellbore, the radial stress, which acts in all direction at right angle to the wellbore, and the axial stress, which acts along the wellbore

axis (Figure 2.4). In deviated wells, shear components exist alongside the previously mentioned redistributed stresses. Wellbore failure will occur when the redistributed stress is higher than the strength of the formation (McLean and Addis 1990).

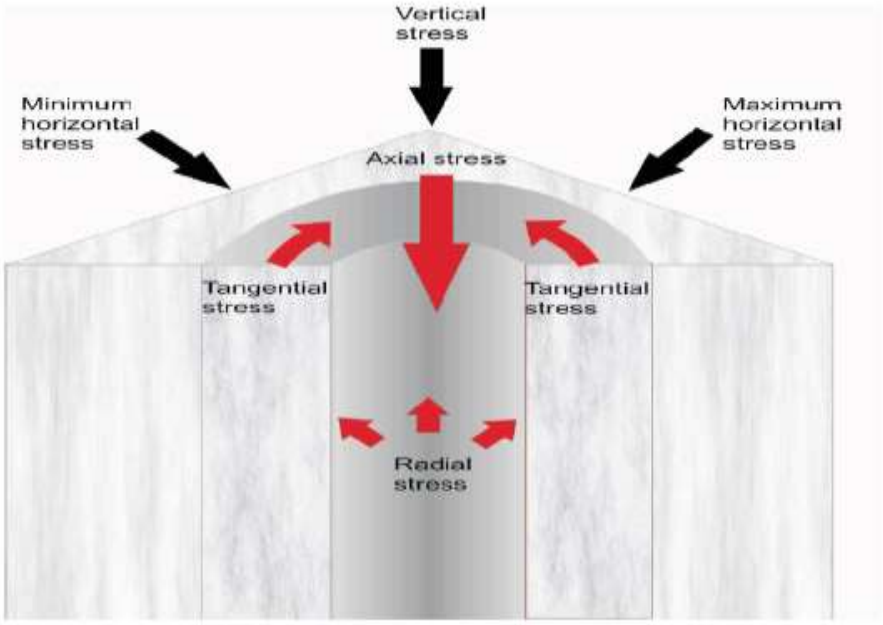

Figure 2.4: Wellbore stresses (Pasic 2007)

Wellbore instability can be ascribed to one or many causes, Pasic et al. 2007 summarized causes of borehole failure as controllable and uncontrollable (natural) factors. Controllable factors include bottom-hole pressure, wellbore inclination and azimuth, transient wellbore pressures (surge and swab), physical/chemical rock-fluid interaction, drill string vibrations, erosion caused by excessive flow rates and drilling fluid temperature. Uncontrollable or natural factors include naturally fractured or faulted

formations, tectonically stressed formations, high in situ stresses, pore pressure, mobile (plastic) formation and unconsolidated formations.

Stress acting around a wellbore is a function of wellbore path, there is higher chances of wellbore instability when drilling deviated and horizontal wells in zones of normal fault regime (overburden is the maximum principal stress). Drilling fluid with temperature lower than that of the formation can lead to reduced stresses around wellbore and drilling fluid with higher temperature induces thermal stresses. Drilling overbalance in fractured low permeability formations like shale and limestone is also a common source of wellbore instability. These rocks fail when pressures in the fractures rises as they are invaded by drilling fluids. This kind of instability can be mitigated if effective sealing agents are added to drilling fluid (Labenski et al. 2003). Tectonically active formations (one of horizontal stress is the maximum principal stress) which is typical of mountainous areas can pose serious challenges when drilling a vertical well, higher hydrostatic pressure may be needed to prevent instability and a deviated or horizontal well might be the optimum well trajectory in these formations.

2.2.2 Types of Wellbore Instability

Wellbore instability can be broadly classified into two types, namely, chemically induced and mechanically induced wellbore instability, and instability may be as a result of both (Xu 2007).

2.2.2.1 Chemically Induced Instability

Chemically induced instability occur as a result of interactions between drilling fluid and the rocks around walls of the wellbore. It alters near wellbore rock properties as

a result of hydration, osmotic pressure, swelling, rock softening and leaching (Pasic 2007 and Xu 2007). A typical example of this type of instability is the hydration of swelling clays in shale. Interaction of water with shale alters the strength and pore pressure, commonly leading to increased pore pressure and decreased strength (Lal 1999). Different clay minerals in shale have varying capacity for adsorption of water because of different surface areas and Cation Exchange Capacity (CEC), adsorbed water causes increase in bulk volume of shale or swelling pressure if shale is not allowed to expand. If rock stays intact after increase in the bulk volume of rock, there will be a reduction in size of wellbore. Conversely, swelling pressure can lead to disintegration of shale, thus causing wellbore enlargement (Cheatham 1984). Another example of chemical instability is leaching of salt formations. Water present in drilling fluid can dissolve part of salt rocks, leading to increased wellbore size. Instability induced chemically can be eased by proper selection of drilling fluid, using additives that can delay or minimize fluid/rock interaction, and by reducing shale exposure time (Lal 1999).

2.2.2.2 Mechanically Induced Instability

Mechanically induced instability occurs when the redistributed stresses exceed the compressive or tensile strength of the near wellbore rocks. The pressure exerted by drilling fluid controls the radial stress at the wellbore wall. A decrease in pressure of drilling fluid leads to an increase in hoop stress at the wellbore wall and an increase in drilling fluid pressure decreases the hoop stress. High hoop stresses around wellbore can lead to compressive failure, while low hoop stresses can lead to tensile failure if the tensile strength of the rock is mobilized. To prevent compressive failure, the wellbore pressure

must be high enough to keep the redistributed stress below the strength of the formation. Bradley (1979) presented three types of stress induced wellbore instability (Figure 2.5), they are:

I. Plastic Failure of the Formation:

Plastic failure of near wellbore rocks result in wellbore size reduction and is caused by compressive failure of the formation. The pressure of the drilling fluid is not sufficient to maintain a stable borehole, leading to high hoop stress. This instability requires the development of a plastic shear strain around the wellbore and some of the shear strength of the rock is lost (Abdulhadi 2009). Weak shale and salt formations are examples of rocks that fail in this manner. Plastic deformation of the formation can lead to stuck pipe, damaged casing during production and may require reaming to get the desired size of wellbore. Increasing the density of drilling fluid can help mitigate plastic failure of the formation.

II. Brittle Failure of the Formation:

Similarly, brittle failure is caused by compressive failure of the formation when the pressure of the drilling fluid is not sufficient to maintain a stable borehole, but leads to enlargement of the wellbore (borehole breakout). It occurs in hard rocks like sandstone and can be used to predict the direction of the minimum horizontal stress. Here, the shear strength of the rocks near the wellbore is mobilized (Abdulhadi 2009). Problems associated with this instability include excessive production of cuttings, poor directional control, poor cementing jobs,

reduced borehole cleaning efficiency, higher pump pressure and loss of the well in the case of a total collapse. Increasing the density of drilling can help mitigate brittle failure of the formation.

III. Tensile Failure of the Formation:

Tensile failure happens when the tensile strength of the formation has been mobilized, typically when the hoop stress becomes tensile. Here, the formation is fractured as a result of reduced hoop stress when the pressure of the drilling fluid is too high. Tensile failure leads to loss of drilling fluid to the formation (lost circulation) and potential well control issues. Well control issues will occur if the wellbore pressure is lower than the formation pressure, the formation has sufficient permeability and there is a mobile fluid in the formation (Watson et al. 2003). Decreasing drilling fluid density prevents tensile failure of the formation.

Wellbore bridging requires the blockage of flow part of formation fluids. Therefore chemically induced instability, plastic failure of the formation and brittle failure of the formation have a potential of causing wellbore bridging. Tensile failure of the formation do not produce large quantity of caving and will not be studied in this work.

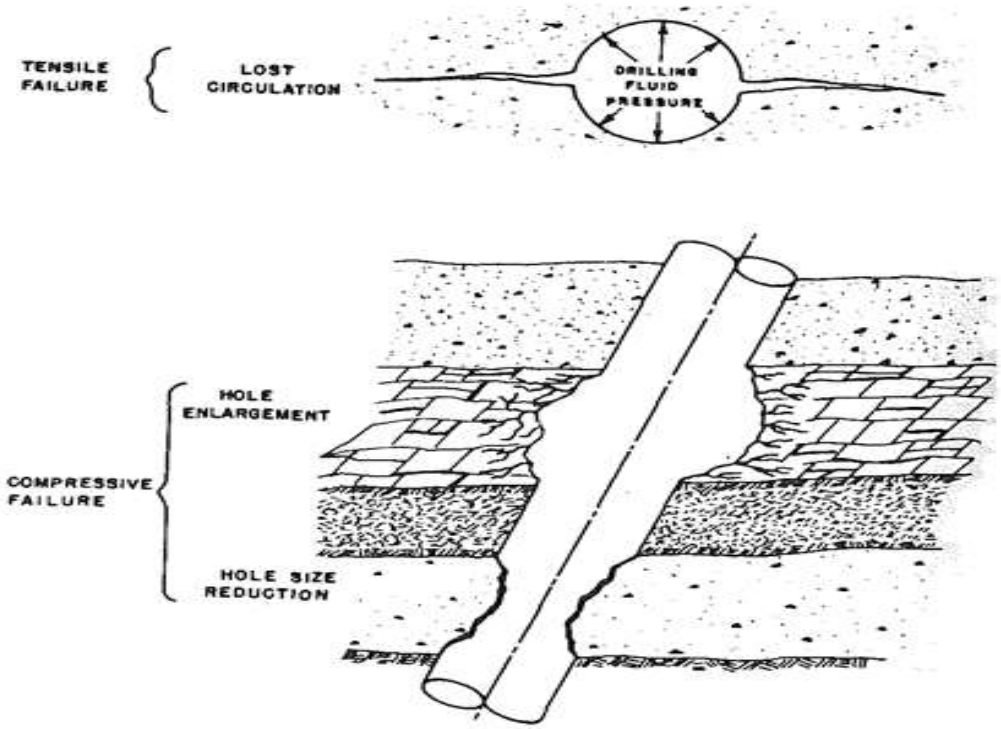

Figure 2.5: Types of wellbore instability (Bradley 1979).

2.2.3 Wellbore Stability Analysis

Wellbore stability analysis involves the determination of the optimum drilling fluid density window to prevent wellbore collapse. There are always tradeoffs when drilling overbalance, underbalance or just balanced. Drilling overbalance can prevent many types of wellbore instability but can adversely affect drilling rates and create an environment for a potential differential pipe sticking. Drilling underbalance comes with an advantage of higher drilling rates but can be plagued with wellbore instability problems especially when drilling in weak formations.

The drilling fluid density is constrained by pore pressure, fracture gradient and wellbore collapse gradient limit presented by the formation. The fracture gradient represents the top limit of the drilling fluid density window, while the lower limit should be set by the pore pressure in hard rocks and or pressure required to prevent wellbore collapse in weak rocks (Akl 2011). In very tight formations or when formation fluid is very viscous, wellbore pressure less than formation pressure might not lead to a well control situation. In this case, the wellbore collapse initial pressure should set the lower limit of the drilling fluid density.

Inputs to a wellbore stability analysis include rock mechanical properties, in situ stresses magnitude and orientation, wellbore trajectory, pore pressure, temperature and failure criteria. The maximum horizontal stress orientation (S_{Hmax}) is often the most challenging parameter to establish for in situ stress assessment, although, this factor does not affect wellbore stability analysis in vertical wells but does affect deviated wells (Li and Bai 2012). Trajectory of wellbore influences the drilling fluid density required to drill a stable well. In areas with normal faults, drilling a deviated well is less favorable because the vertical stress will have an increased component normal to the wellbore, hence, higher mud weight will be required to maintain a stable wellbore. Conversely, in tectonically stressed area, increased deviation in a given azimuth direction will be more favorable (Akl 2011). Pore pressure has an impact on the effective stress which a rock is subjected to, increasing pore pressure reduces effective stress and moves the effective stress circle toward the failure envelope. This increases the density of drilling fluid required to sustain a stable borehole as pore pressure increases.

Several works has been done in the area of wellbore stability, and typically, the formation around the wellbore is assumed to be a linear elastic body (Bradly 1979, McLean and Addis 1990). Wellbore failure is dependent on rock failure criterion and the stress-strain behavior (model) selected to determine the response of formation to loading. The model is used to estimate the stress and strain around the wellbore and the strength of the rock is described using a selected failure criterion.

A model can be purely elastic or elasto-plastic with one or more effects (pore pressure, chemical, thermal) taken into account. In elasto-plastic models, plastic deformation occur when a certain yield criterion is reached. Elasto-plastic models are more representative since most rocks hardly behave perfectly elastic to ultimate failure but they are more complex than the elastic models and not easy to apply. Failure criteria are used to determine if failure has occurred and a particular criterion is more suitable for some type of rocks. For example, Mohr-Coulomb failure criterion is more suitable for sandstone formation while the modified Lade failure criterion is most accepted for shale formations (McLean and Addis 1990, Li and Bai 2012, Kang et al. 2009).

The input parameters used for wellbore stability analysis are estimates and are only known with some level of certainty. The quality of wellbore instability analysis is dependent on the accuracy of it input parameters. Li and Bai (2012) performed a sensitivity analysis to determine the input parameter (in situ stress state, rock properties and selected failure criterion) whose accuracy affect the output of wellbore stability analysis the most. Their investigation showed that the accuracy of the minimum horizontal stress (S_{hmin}) is the most critical parameter when defining the optimum drilling fluid density required to

prevent wellbore collapse due to shear failure. Other examined parameters in decreasing order of sensitivity are unconfined compressive strength (UCS), pore pressure, maximum horizontal stress, vertical stress, azimuth of maximum horizontal stress and breakout angle.

In conclusion, estimated depth by depth optimum drilling fluid densities will show that one drilling fluid density cannot be used to drill a well from top to bottom. Upper parts of the well need to be protected using casing strings if the present mud weight can fracture them. This process is repeated until total depth is reached.

2.3 Wellbore Strengthening Effect

2.3.1 Filter Cake Effect

Formation strengthening by drilling fluids has been discussed extensively in the literature and have been described with many terms that includes fracture closure stress, fracture plugging/sealing and internal filter cake bridging (Abousleiman et al. 2007, Fett et al. 2009). Aadnoy et al. 2008 designed and tested a drilling mud which they found to strengthen the formation by increasing the mud loss gradient. In their work they reported that the formation fractures before mud cake collapses and mud cake forms a bridge over the fracture, hence, increasing the rock's strength. Studies of mechanical properties of mud cake showed that mud cake behaves elastically with wellbore pressure and elastic failure is not likely for mud cake. Failure of mud cake will occur at a higher pressure level and mud cake thickness can be as high as 10mm (Mostafavi et al. 2010).

2.3.2 Temperature Effect

As drilling fluid is circulated top-bottom through the drill string and bottoms-up through the annulus, it experiences an increase in temperature top-bottom and then a decrease in temperature bottom-up. Formation is hotter than the drilling fluid at the bottom and colder above the neutral point (same temperature at the neutral point). As a result of this temperature difference, the formation is either being heated or cooled depending on the depth of consideration leading to pore pressure changing and expansion or contraction of rock grains and pore fluids. Consequently, the stress profile around the wellbore is altered (Kang et al. 2009).

Heating the formation induces compressive stresses while cooling induces tensile stresses. A temperature difference of 1^{o}C can cause 0.4 to 1 MPa tensile or compressive stress, depending on the stiffness of the rock (Nesheli 2006). Tran (2010) reported drilling induced closely-spaced transverse fractures that are perpendicular to wellbore axis in horizontal wells detected by micro-imaging logs. Analysis showed that wellbore stability models that ignored thermal effect could not explain these phenomenon. Further investigation showed that, for a horizontal well in the Barnett, thermal effect due to about 30^{o}C temperature difference (drilling fluid cooler) can cause tensile failure detected by the micro-imager log despite the high strength of the formation. Similarly, Guenot and Santarelli (1989) discussed thermal induced wellbore instability in their field case study. They reported formation spalling as a result of heating and drilling induced fractures as a result of formation cooling and estimated that a cooling of 20^{o}C caused a reduction of 10MPa in hoop stress.

Furthermore, several thermo-poro-elastic models have shown that thermally induced stresses have an effect on wellbore stability analysis. Ignoring the effect of temperature difference can lead to inaccurate prediction of optimum drilling fluid density. Chen and Ewy (2005), Choi and Tan (1998), and Li et al. (1998) in their various works modelled thermal effect using thermo-poro-elastic models. They concluded that cooling the formation reduces formation spalling and heating enhances wellbore breakout.

2.4 Rock Compressive Strength Criteria

It is more difficult to crush a rock than for rock grains to slide past one another, hence when rocks fail in compression, they fail in shear because of inter-granular slip. Resistance to shear or shear strength is a function of cohesion and friction between the rock grains (Lal 1999). Wellbore failure is dependent on rock failure criterion and the stress-strain behavior (model) selected to determine the response of formation to loading. Selected rock compressive strength criteria is an important factor during wellbore stability analysis. Failure criteria selected for stability analysis plays a huge role on the output of the analysis. Many criteria have been developed based on lab tests to define rock strength under various stress settings. Mohr-Coulomb failure criteria is commonly used but it disregards the effect of the intermediate principal stress, as a result, its parameters can be determined from standard triaxial test ($\sigma_1 > \sigma_2 = \sigma_3$) (Zoback 2007). Polyaxial criteria such as modified Lade and Drucker-Prager considers the effect of σ_2.

2.4.1 Mohr-Coulomb Failure Criterion

It is appropriate to characterize rock strength using Mohr-Coulomb failure criterion when σ_2 is slightly greater than or equal to σ_3 (Bejarbaneh et al. 2015). This criterion works well for strong rocks. To describe shear failure using this criterion requires the determination of the Mohr-Coulomb parameters S_0 and ϕ. These parameters are determined experimentally by testing rocks to failure in a triaxial setup at different confining stress and then constructing a Mohr-Coulomb failure envelope (Figure 2.6) from results of the test. Any circle above the failure line means failure will occur, while circles below the line implies absence of failure. Mohr-Coulomb failure criterion is commonly expressed in the forms below:

$$\tau = S_0 + \sigma'_n \mu \tag{2.1}$$

From the Mohr-Coulomb failure envelope (Figure 2.6), the following can be deduced (Fjaer et al. 2008):

$$\tau = \frac{1}{2}(\sigma_1 - \sigma_3)\sin 2\beta \tag{2.2}$$

$$\sigma'_n = \frac{1}{2}(\sigma'_1 + \sigma'_3) + \frac{1}{2}(\sigma'_1 - \sigma'_3)\cos 2\beta \tag{2.3}$$

$$\beta = 45° + \frac{\phi}{2} \tag{2.4}$$

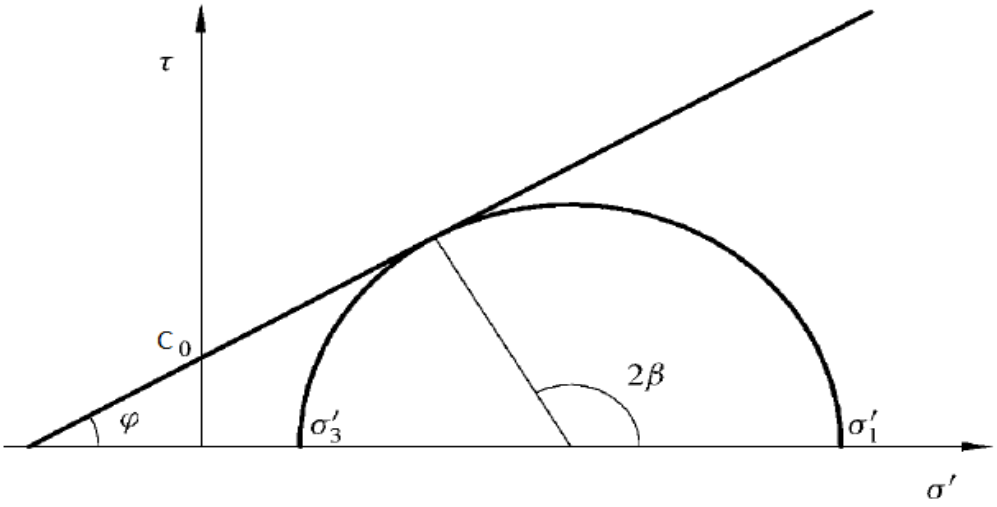

Figure 2.6: Mohr-Coulomb failure envelope (Fjaer et al. 2008).

Substituting equations 2.2 - 2.4 into 2.1 and simplifying results in;

$$\sigma_1' = 2S_0 \frac{\cos\phi}{1-\sin\phi} + \sigma_3' \frac{1+\sin\phi}{1-\sin\phi} \tag{2.5}$$

$$\mathrm{UCS} = 2S_0 \frac{\cos\phi}{1-\sin\phi} \tag{2.6}$$

$$\sigma_1' = \mathrm{UCS} + \sigma_3' \left(\frac{1+\sin\phi}{1-\sin\phi}\right) \tag{2.7}$$

where

τ = Shear stress required to cause failure along failure plane

S_0 = Cohesion

σ_n' = Effective normal stress acting on failure plane

μ = Coefficient of internal friction ($\tan\phi$)

σ_1' = Effective maximum principal stress

σ_3' = Effective minimum principal stress

ϕ = Angle of internal friction

Equation 22.7 gives an expression for calculating the value of one of the principal stresses required to cause failure when the value of the other is fixed.

2.4.2 Drucker-Prager Failure Criterion

The Drucker-Prager failure criterion is a polyaxial criteria because it considers the effect of intermediate principal stress on the rock strength. It is also called the extended von Mises yield criterion and was initially developed for soil mechanics. The Drucker-Prager criterion can be expressed as:

$$J_2^{1/2} = k + \alpha J_1 \tag{2.8}$$

$$J_1 = \frac{1}{3}(\sigma_1' + \sigma_2' + \sigma_3') \tag{2.9}$$

$$J_2 = \frac{1}{6}[(\sigma_1' - \sigma_2')^2 + (\sigma_1' - \sigma_3')^2 + (\sigma_2' - \sigma_3')^2] \tag{2.10}$$

where k and α are material constants that can be related to the Mohr-Coulomb parameter (S_o and ϕ). Setting α to zero reduces the Drucker-Prager failure criterion to the von Mises criterion. The Drucker-Prager criterion can be classified as Circumscribed Drucker-Prager or Inscribed Drucker-Prager criterion depending on its relationship with the Mohr-Coulomb criterion (Zoback 2007). The Circumscribed Drucker-Prager circle touches the outer tips the Mohr-coulomb yield surface and it material constants are expressed as:

$$\alpha = \frac{6\sin\phi}{\sqrt{3}(3-\sin\phi)} \tag{2.11}$$

$$k = \frac{6 S_o \cos\phi}{\sqrt{3}(3-\sin\phi)} \tag{2.12}$$

The Inscribed Drucker-Prager circle touches the inside of the Mohr-coulomb yield surface and it material constants are expressed as:

$$\alpha = \frac{3\sin\phi}{\sqrt{9+3(\sin\phi)^2}} \tag{2.13}$$

$$k = \frac{3\,S_o\cos\phi}{\sqrt{9+3(\sin\phi)^2}} \tag{2.14}$$

2.4.3 Modified Lade Failure Criterion

The Lade criterion is a 3D criterion firstly developed for frictional materials without effective cohesion, the criterion works well with weak rocks and those rocks whose strength strongly depends on the intermediate principal stress (Zoback 2007). The Modified Lade criterion is a modified version of the Lade criterion developed by Ewy (1999). Ewy (1999) argued that the two most widely used failure criteria for wellbore stability analysis, Mohr-Coulomb and Drucker-Prager, represented two extreme treatments of the intermediate principal stress, with the Mohr-Coulomb criterion ignoring effect of the intermediate principal stress and the Drucker-Prager criterion ascribing the same weight to the intermediate principal stress as the maximum and minimum principal stresses. The Lade criterion can be written as:

$$\left(\frac{I_1^3}{I_3} - 27\right)\left(\frac{I_1}{P_a}\right)^m = \eta_1 \tag{2.15}$$

$$I_1 = \sigma_1 + \sigma_2 + \sigma_3 \tag{2.16}$$

$$I_3 = (\sigma_1)(\sigma_2)(\sigma_3) \tag{2.17}$$

The parameter P_a is atmospheric pressure, while η_1 and m are material constants.

Ewy (1999) modified this criterion by setting m = 0 to predict linear shear strength increase with I_1, introduced a new term S_1 so the criterion can handle materials with cohesion or a non-tensile strength and pore pressure to handle effective stresses. The modified criterion can be written as:

$$\frac{(I_1'')^3}{I_3''} = \eta + 27 \tag{2.18}$$

$$I_1'' = (\sigma_1 + S_1 - P_0) + (\sigma_2 + S_1 - P_0) + (\sigma_3 + S_1 - P_0) \tag{2.19}$$

$$I_3 = (\sigma_1 + S_1 - P_0)(\sigma_2 + S_1 - P_0)(\sigma_3 + S_1 - P_0) \tag{2.20}$$

where η and S_1 are material constant related to the Mohr-Coulomb parameter (S_o and ϕ) by:

$$\eta = \frac{4(\tan\phi)^2(9-7\sin\phi)}{(1-\sin\phi)} \tag{2.21}$$

$$S_1 = \frac{S_o}{\tan\phi} \tag{2.22}$$

Because S_1 and η are can be related to the Mohr-Coulomb parameters, this criterion is easy to use in practice.

CHAPTER III

EVALUATION OF FAILURE CRITERIA

3.1 Stress Concentrations around a Cylindrical Wellbore

Redistributed stress acting around an elastic and isotropic vertical wellbore is described by the Kirsch equations. Using the plain strain approximation and setting induced shear stresses as zero, these equations for a vertical wellbore with radius R can be written in the following form (Aadnoy and Looyeh 2011, Chi et al. 2013, Zoback 2007):

$$\sigma'_{rr} = \frac{1}{2}(S_{Hmax} + S_{hmin} - 2P_o)\left(1 - \frac{R^2}{r^2}\right) + \frac{1}{2}(S_{Hmax} - S_{hmin})\left(1 - \frac{4R^2}{r^2} + \frac{3R^4}{r^4}\right)\cos 2\theta + (P_w - P_o)\frac{R^2}{r^2} - \sigma_{rr}^{\Delta T} \quad (3.1)$$

$$\sigma'_{\theta\theta} = \frac{1}{2}(S_{Hmax} + S_{hmin} - 2P_o)\left(1 + \frac{R^2}{r^2}\right) - \frac{1}{2}(S_{Hmax} - S_{hmin})\left(1 + \frac{3R^4}{r^4}\right)\cos 2\theta - (P_w - P_o)\frac{R^2}{r^2} - \sigma_{\theta\theta}^{\Delta T} \quad (3.2)$$

$$\sigma'_{zz} = S_v - 2\upsilon(S_{Hmax} - S_{hmin})\left(\frac{R^2}{r^2}\right)\cos 2\theta - P_o - \sigma_{zz}^{\Delta T} \quad (3.3)$$

where

σ'_{rr} = Effective radial stress

$\sigma'_{\theta\theta}$ = Effective hoop stress

σ'_{zz} = Effective axial stress along wellbore axis

P_o = Formation pore pressure

P_w = Wellbore pressure

θ = Angle around wellbore measured from S_{Hmax}

υ = Poisson's Ratio

r = Radial distance into formation from wellbore center (r = R at wellbore wall)

$\sigma_{rr}^{\Delta T}$ = Thermally induced radial stress

$\sigma_{\theta\theta}^{\Delta T}$ = Thermally induced hoop stress

$\sigma_{zz}^{\Delta T}$ = Thermally induced axial stress

For plain stress approximation, σ'_{rr} and $\sigma'_{\theta\theta}$ remain the same but σ'_{zz} is expressed as:

$$\sigma'_{zz} = S_v \tag{3.4}$$

For wellbore collapse analysis, the hoop stress is the maximum principal stress, axial stress is the intermediate principal stress and radial stress is the minimum principal stress.

3.2 Thick-Walled Cylinder Test

Thick-Walled Cylinder (TWC) tests are widely used in the laboratory to simulate stresses around a wellbore and study onset of collapse in a hollow cylinder rock sample with circular cross-section. These hollow samples are subjected to stresses identical to those in situ and can be used to validate numerical simulations (Wu et al. 2000). Typically, The procedure for performing TWC test are sample preparation and installation, back pressure saturation, consolidation and shearing (borehole pressure reduction) of specimen (Marsden and Dennis 1996, Wu et al. 2000, Abdulhadi et al. 2011, Gabrielsen et al. 2011).

Results of TWC from six works (Abdulhadi 2009, Islam and Skalle 2011, Marsden and Dennis 1996, Nes et al. 2015, Gabrielsen et al. 2010, Salisbury et al. 1991) were gathered for analysis. It should be noted that all of these tests were performed on shale samples. Abdulhadi 2009 did not have values of yield pressure expressly stated. The values of the yield pressure for this work was read from a graph as the cavity pressure at which the shear strength was mobilized at the borehole wall. Collapse initiation pressure were calculated for all tests using four failure criteria and the results compared to those obtained from experiments. The failure criterion used are Mohr-Coulomb (MC), Modified Lade (ML), Inscribed Drucker-Prager (IC DP) and Circumscribed Drucker-Prager (CS DP). The analysis was performed using the Kirsch's equation for wellbore with circular cross-section.

3.3 Result of Failure Criteria Evaluation

Table 3.1 shows the information extracted from six works and computed values of collapse initiation pressure for the different tests. All test were conducted using equal horizontal stresses. The plain strain and plain stress approximations were both used for collapse initiation pressure computations for tests 1, 2, 5 and 7, while the plain stress approximation was used for tests 3, 4, 6, and 8 to 13 because the values of the Poisson's Ratio were not available for the rock sample in the sources. It should be noted that both the plain stress and plain strain approximations gave the same results for the analysis because both horizontal stresses are equal. The values of the computed collapse initiation pressure should be compared to the yield pressure when available because the various

criteria used are yield criteria and elastic model was used, they calculate on set of collapse which is analogous to the yield pressure.

Generally, the computed collapse initiation pressure using the four failure criterion gave somewhat similar results and correlated well with those obtained from the experiments. The results computed using the Inscribed Drucker-Prager criterion seems to be the least accurate among all four criteria and consistently gave the highest difference between computed and experimental results. The Circumscribed Drucker-Prager predicted the strongest rock (lowest collapse pressure) among all four failure criteria and gave collapse initiation pressure closest to those obtained in the experiments.

During this analysis, some convergence problems were encountered with the Inscribed Drucker-Prager failure criterion. The colored part of the table show when these instabilities occurred. Whenever these instabilities occurs, the accuracy of the solver needs to be reduced to get a solution. The yellow spots show when accuracy was only reduce slightly, while the red spots shows when accuracy was largely reduced.

Test		1	2	3	4	5	6	7
Source		Islam and Skalle 2011	Islam and Skalle 2011	Marsden et al. 1996	Marsden et al. 1996	Nes 2015	Gabrielsen et al. 2010	Salisbury et al. 1991
*Axial Stress (MPa)		30.00	30.00	30.00	20.00	39.00	-	31.00
*Confining stress (MPa)		30.00	30.00	30.00	20.00	39.00	15.00	29.00
*Pore Pressure (MPa)		25.00	25.00	20.00	15.00	32.00	10.00	28.30
*Angle of Internal Friction (°)		27.90	26.00	15.00	15.00	1.00	19.00**	20.05
*Cohesion (MPa)		3.10	3.00	0.59	0.59	3.78	4.39	0.55
*Young's Modulus (GPa)		2.60	1.55	-	-	0.80	-	3.50
*Poisson's Ratio		0.29	0.52	-	-	0.40	-	0.36
*Yield Pressure (MPa)		-	-	28.60	17.20	30.00	7.70	-
*Collapse Pressure (MPa)		22.40	19.0	24.90	15.50	-	3.30	24.80
Calculated P_{ci} (MPa)	IC DP	25.10	25.26	26.88	18.16	35.10	9.32	29.00
	MC	24.92	25.11	26.84	18.14	35.10	9.22	28.24
	ML	23.97	24.19	26.27	17.80	34.49	8.15	28.60
	CS DP	23.05	23.39	26.01	17.64	34.47	7.52	28.44

Table 3.1: Collapse initiation pressure comparison (Experiment vs Calculated).
- Information not available in source
* Data from experiment
** Data from Shewalla, M. (2007)
IC DP - Inscribed Drucker-Prager MC - Mohr-Coulomb
ML - Modified Lade CS DP - Circumscribed Drucker-Prager
P_{ci} – Collapse Initiation Pressure

Test		8	9	10	11	12	13
Source		Abdulhadi 2009					
*Axial Stress (MPa)		10.20	2.95	5.88	1.47	1.47	1.48
*Confining stress (MPa)		5.61	1.62	3.23	1.47	0.81	0.81
*Pore Pressure (MPa)		0.65	0.50	0.42	0.62	0.46	0.40
*Angle of Internal Friction (°)		26.81	26.81	26.81	26.81	26.81	26.81
*Cohesion(MPa)		0.33	0.09	0.19	0.05	0.05	0.05
*Young's Modulus (GPa)		1.02	0.41	0.76	0.27	0.27	0.27
*Poisson's Ratio		-	-	-	-	-	-
*Yield Pressure (MPa)		2.60	1.10	1.20	0.88	0.58	0.48
*Collapse Pressure (MPa)		-	-	-	-	-	-
Calculated P_{ci} (MPa)	IC DP	3.97	1.60	2.33	1.06	0.73	0.75
	MC	3.08	1.03	1.80	1.05	0.61	0.58
	ML	3.16	1.11	1.85	0.97	0.72	0.66
	CS DP	2.13	0.87	1.26	0.89	0.67	0.58

Table 3.1 continued.

CHAPTER IV

METHODOLOGY

Mostafavi et al. (2010) gave an expression for hoop and radial stress for equal horizontal stresses at the surface of the formation in the presence of mud cake as:

$$\sigma_{\theta\theta} = \left(1 + \frac{r_{mc}^2}{r_w^2}\right)\sigma_h - \left(\frac{r_{mc}^2}{r_w^2}\right)P_w \tag{4.1}$$

$$\sigma_{rr} = \left(1 - \frac{r_{mc}^2}{r_w^2}\right)\sigma_h + \left(\frac{r_{mc}^2}{r_w^2}\right)P_w \tag{4.2}$$

where

$\sigma_{\theta\theta}$ = Hoop stress

P_w = Wellbore Pressure

σ_h = Horizontal stress

r_{mc} = Wellbore radius to mud cake interface

T_{mc} = Mud cake thickness

r_w = Wellbore radius to formation wall

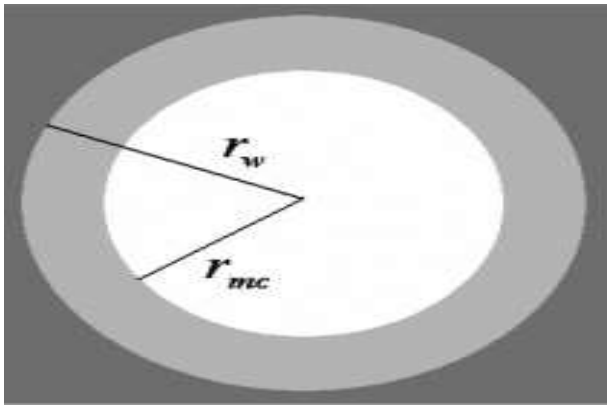

$$r_{mc} = r_w - T_{mc}$$

Figure 4.1: Mud cake attached to formation (Mostafavi et al. 2010).

In their work, they assumed constant filter cake thickness and that the mud cake was a part of the formation but with different properties, hence the wellbore pressure is applied on the filter cake (Figure 4.1). They varied values of both the isothermal compressibility and the filter cake thickness to study how the hoop stress is affected when mud cake is present cake assuming equal values of in situ horizontal stresses.

This work will be using a similar approach with unequal horizontal stresses to see how factors such as wellbore size, mud cake thickness and compressibility, rock unconfined compressive strength, stress state and stress magnitude will affect the wellbore collapse initiation pressure. Using a similar concept as Mostafavi et al. (2010) and assuming plain strain condition, the effective radial, hoop and axial stresses at the surface of the formation can be expressed in the following format using unequal horizontal stresses and including thermally induced stresses:

$$\sigma'_{rr} = \frac{1}{2}(S_{Hmax} + S_{hmin} - 2P_o)\left(1 - \frac{r_{mc}^2}{r_w^2}\right) + \frac{1}{2}(S_{Hmax} - S_{hmin})\left(1 - \frac{4r_{mc}^2}{r_w^2} + \frac{3r_{mc}^2}{r_w^2}\right)\cos 2\theta + (P_w - P_o)\frac{r_{mc}^2}{r_w^2} - \sigma_{rr}^{\Delta T} \tag{4.3}$$

$$\sigma'_{\theta\theta} = \frac{1}{2}(S_{Hmax} + S_{hmin} - 2P_o)\left(1 + \frac{r_{mc}^2}{r_w^2}\right) - \frac{1}{2}(S_{Hmax} - S_{hmin})\left(1 + \frac{3r_{mc}^2}{r_w^2}\right)\cos 2\theta - (P_w - P_o)\frac{r_{mc}^2}{r_w^2} - \sigma_{\theta\theta}^{\Delta T} \tag{4.4}$$

$$\sigma'_{zz} = S_v - 2\upsilon(S_{Hmax} - S_{hmin})\left(\frac{r_{mc}^2}{r_w^2}\right)\cos 2\theta - P_o - \sigma_{zz}^{\Delta T} \tag{4.5}$$

Instead of using random values of isothermal compressibility, mud cake parameters as introduced by Dewan and Chenevert (2001) will be used. These parameters have been shown to effectively capture the behavior of mud cake (Calçada et al. 2014). Expressions from Dewan and Chenevert (2001) relevant to this work are:

$$\emptyset_{mc} = \frac{\emptyset_{mc0}}{P_{mc}^{\delta c}} \tag{4.6}$$

where

$\emptyset_{mc}$ = Mud cake Porosity at P_{mc}

$\emptyset_{mc0}$ = Reference mud cake porosity

δ = A multiplier with values between 0.1 - 0.2

c = Compressibility exponent

c = 0 represent incompressible mud cake and c = 1 represent very compressible cake. When pressure changes from P_{mc1} to P_{mc2}, then mud cake thickness will change from T_{mc1} to T_{mc2} according to:

$$T_{mc2} = T_{mc1}\frac{1-\emptyset_{mc1}}{1-\emptyset_{mc2}} \tag{4.7}$$

The parameter P_{mc1} is the mud cake pressure at the initial mud cake thickness and initial porosity, while P_{mc2} is the mud cake pressure at final mud cake thickness when wellbore collapses.

Furthermore, the effect of temperature on collapse initiation pressure when mud cake is present will be considered using an expression for thermal stress variation into the formation by Chi et al. (2013). Using these thermal stresses variation, the radial, hoop and axial stresses at the formation surface when mud cake is present can be expressed as:

$$\sigma_{rr}^{\Delta T} = -\frac{E\alpha}{2(1-\upsilon)}\Delta T\left(1-\frac{r_{mc}^2}{r_w^2}\right) \quad (4.8)$$

$$\sigma_{\theta\theta}^{\Delta T} = \frac{E\alpha}{2(1-\upsilon)}\Delta T\left(1+\frac{r_{mc}^2}{r_w^2}\right) \quad (4.9)$$

$$\sigma_{zz}^{\Delta T} = \frac{E\alpha}{(1-\upsilon)}\Delta T \quad (4.10)$$

where

$\sigma_{rr}^{\Delta T}$ = Induced thermal radial stress

σ_{θ} = Induced thermal hoop stress

σ_{z} = Induced thermal axial stress

E = Young's Modulus

α = Coefficient of Linear thermal expansion

ΔT = Temperature difference between wellbore fluid and formation.

υ = Poisson's Ratio

It should be noted that ΔT is positive (+ve) for wellbore cooling and negative (-ve) for wellbore heating.

Finally, the Mohr-Coulomb, Modified Lade, Inscribed Drucker-Prager and Circumscribed Drucker-Prager failure criteria will be used in the collapse initiation pressure determination. The various criteria behavior with temperature and mud cake will be studied.

This work will be simulating a 12.5 inches hypothetical wellbore with pore pressure gradient of 0.53 psi/ft, overburden gradient of 1.101 psi/ft and minimum horizontal stress gradient of 0.6982 psi/ft with formation rock having angle of internal friction of 35^0 at 5000 ft. The Poisson's ratio of sandstone varies between 0.066 and 0.3

(Watson et al. 2003), for this work, the Poisson's Ratio is assumed to be 0.2 throughout the study and unconfined compressive strength of 7000 psi will be used for most part of the study unless stated otherwise. Using this procedure, a sensitivity analysis of how different variables will impact effect of mud cake on collapse initiation pressure was performed and the results will be discussed in the next chapter. It should be noted that 0^0 is the direction of maximum horizontal stress and 90^0 is the direction of minimum horizontal stress. The minimum horizontal stress direction represent point of maximum compression, where breakouts will start occurring from. Hence, the peak of wellbore profile is expected to be at 90^0.

CHAPTER V

SENSITIVITY ANALYSIS: EFFECT OF MUD CAKE ON COLLAPSE INITIATION PRESSURE

5.1 Effect of Reference Mud Cake Porosity ($\emptyset_{mc0}$) and Initial Mud Cake Pressure (P_{mc1})

The reference mud cake porosity is one of the mud cake parameters used to characterize the behavior of mud cake (Dewan and Chenevert 2001). The value of $\emptyset_{mc0}$ was varied between 0.2 and 0.6, and it corresponding impact on collapse initiation pressure is shown in Figure 5.1 using the Mohr-Coulomb failure criterion. The chart shows the collapse initiation pressure (P_{ci}) plotted for all positions around the wellbore at a fixed depth (wellbore collapse initiation pressure profile) and it can be seen that the collapse initiation pressure is not affected by the reference porosity. The difference between the highest and lowest profile peaks (collapse initiation pressure at 90^0) is less than 8 psi.

Also, the value of initial mud cake pressure was varied to see how it impacts the computed collapse initiation pressure. The initial mud cake pressure is the pressure at which the initial mud cake thickness was measured. Formation of filter cake requires wellbore pressure greater than pore pressure and mud pressure should be lower than the least principal stress to avoid fracturing of the formation, so the value of initial pressure (P_{mc1}) was varied between the pore pressure and the least principal stress. Figure 5.2 shows the wellbore profile using the Mohr-Coulomb failure criterion at different initial mud cake pressure. The chart shows that P_{mc1} has minimal effect on the collapse initiation

pressure. Furthermore, other failure criteria were used (one shown in figure 5.3), and they produced similar results.

This analysis suggest the compressibility of the mud cake has little impact on the collapse initiation pressure but this will be confirmed in subsequent analysis. For subsequent analyses, a value of 0.39 will be used for $\emptyset_{mc0}$ and 3000 psi for P_{mc1} unless stated otherwise.

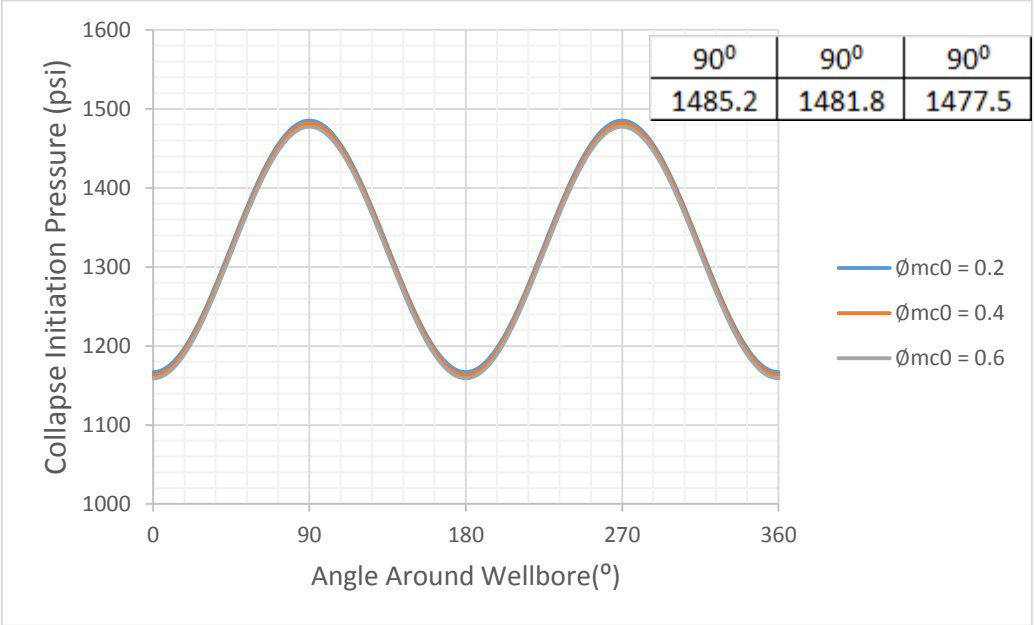

Figure 5.1: Wellbore profile showing effect of reference mud cake porosity on collapse initiation pressure using Mohr-Coulomb failure criterion.
*The peak values (90^0) are in same order as the legend.

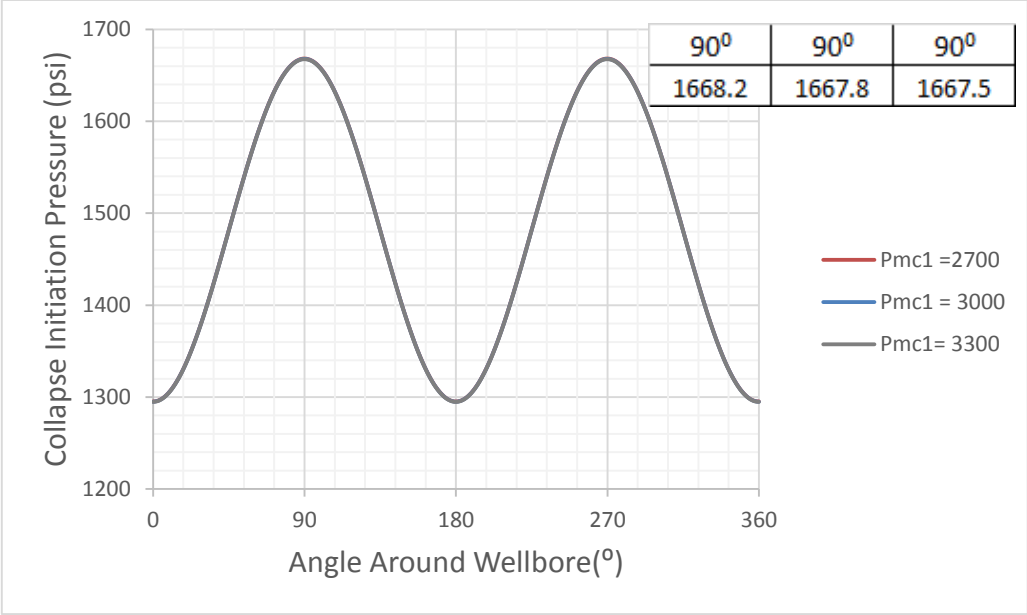

Figure 5.2: Wellbore profile showing effect of initial mud cake pressure on collapse initiation pressure using Mohr-Coulomb failure criterion.

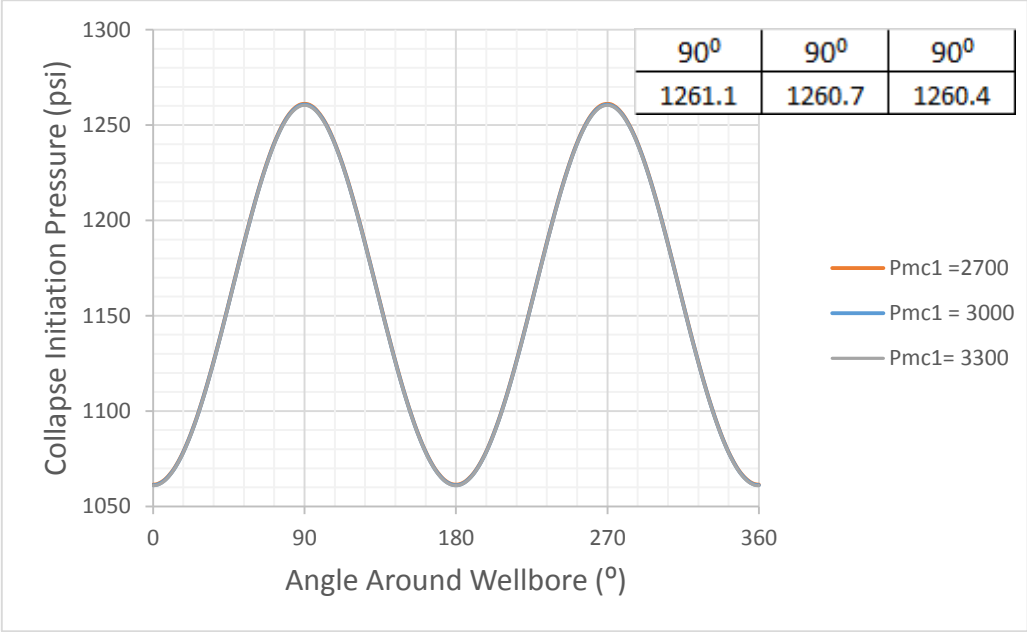

Figure 5.3: Wellbore profile showing effect of initial mud cake pressure on collapse initiation pressure using Modified Lade failure criterion.

5.2 Effect of Mud Cake Compressibility

The compressibility exponents was varied between 0 and 1. Both values represent the two extreme, with 0 signifying completely incompressible and 1 representing very compressible mud cake. Figure 5.4 - 5.6 shows the wellbore profile when mud cake compressibility exponents is 0 and 1 at different values of mud cake thickness. From the charts, it can be deduced that the mud cake compressibility has minimal effect on the collapse initiation pressure. All failure criteria used all showed similar trend (figure 5.7). The difference between collapse initiation pressures at point of maximum compression was less than 1psi when T_{mc} is 2.5 mm and 6 psi when T_{mc} is 10 mm for the Mohr-Coulomb failure criterion and about 10 psi when T_{mc} is 10 mm for Modified Lade failure criterion.

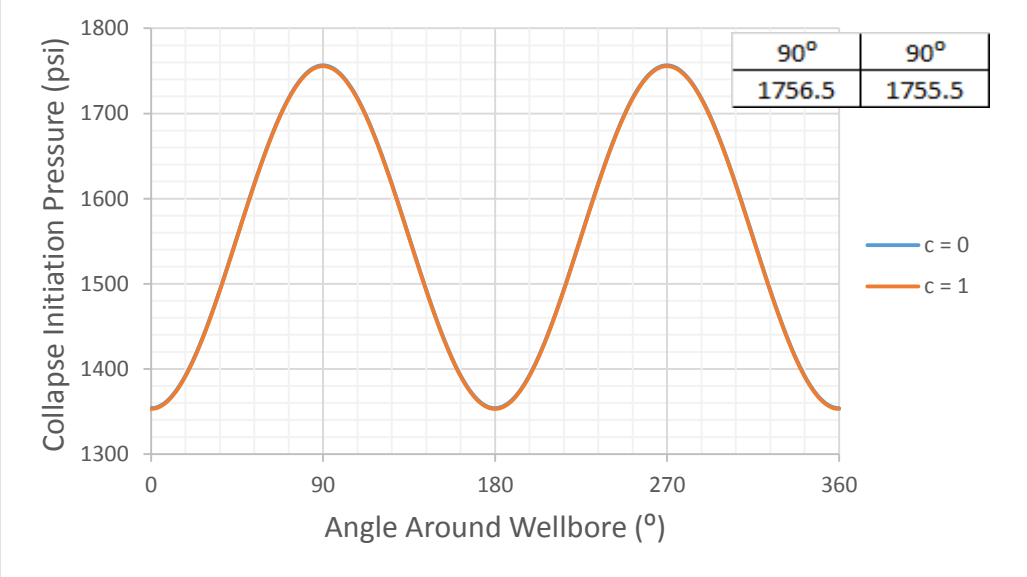

Figure 5.4: Wellbore profile showing effect of compressibility exponent on collapse initiation pressure using Mohr-Coulomb failure criterion when mud cake thickness is 2.5 mm.

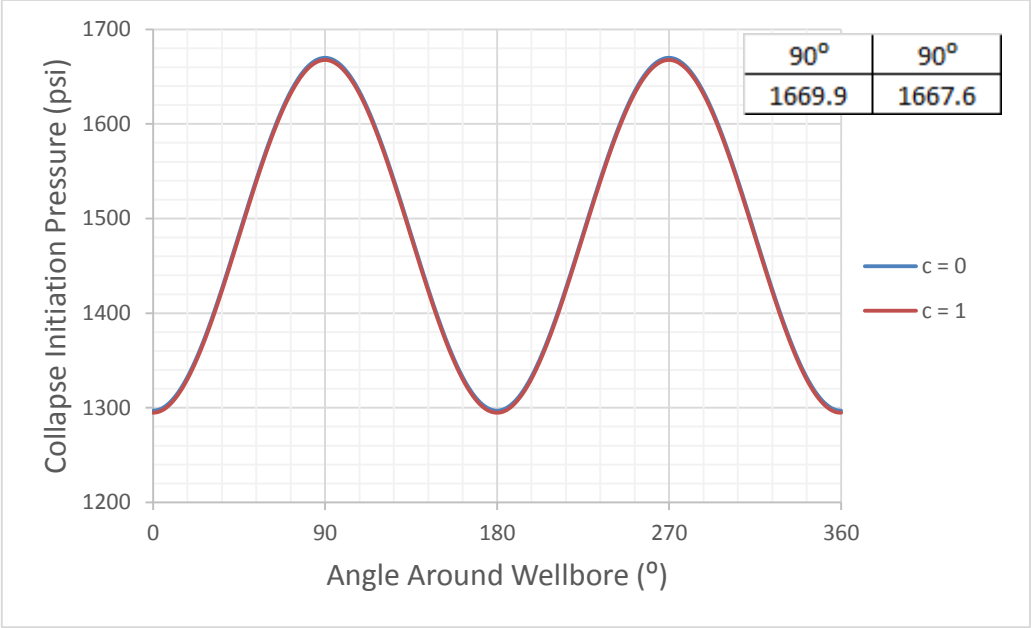

Figure 5.5: Wellbore profile showing effect of compressibility exponent on collapse initiation pressure using Mohr-Coulomb failure criterion when mud cake thickness is 5 mm.

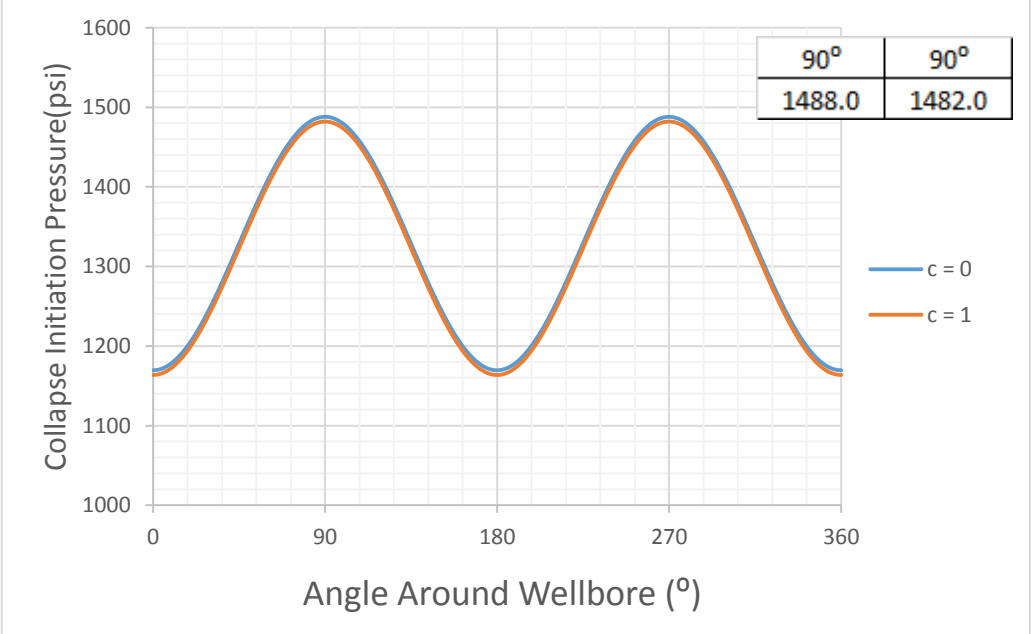

Figure 5.6: Wellbore profile showing effect of compressibility exponent on collapse initiation pressure using Mohr-Coulomb failure criterion when mud cake thickness is 10 mm.

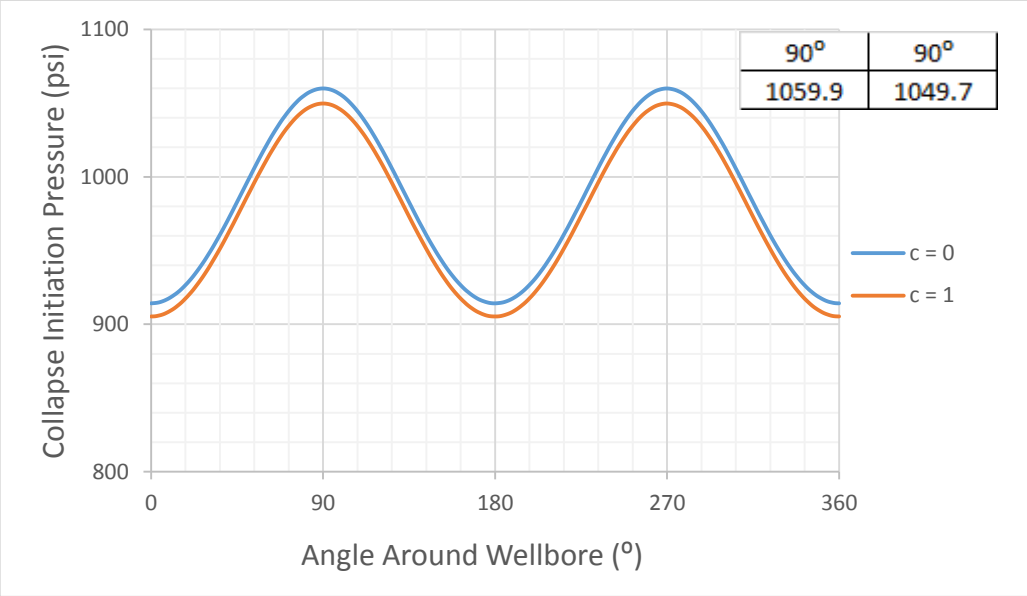

Figure 5.7: Wellbore profile showing effect of compressibility exponent on collapse initiation pressure using Modified Lade failure criterion when mud cake thickness is 10 mm.

5.3 Effect of Mud Cake Thickness

The initial mud cake thickness was varied between 0 and 10 mm and its effect on collapse initiation pressure shown in Figure 5.8 using the Mohr-Coulomb failure criterion and Figure 5.9 using the Modified Lade failure criterion. The results shown are for compressibility exponent of 0 and the ones for other compressibility exponents will be omitted because they show similar results. It can be seen from the charts that the collapse initiation pressure decreases with increase in mud cake thickness, implying that the formation becomes more resistant to collapse with increase in mud cake thickness. For T_{mc} = 10 mm, the point of maximum compression in the case simulated got stronger by about 350 psi when using the Mohr-Coulomb failure criterion and about 400 psi stronger when using the Modified Lade criterion.

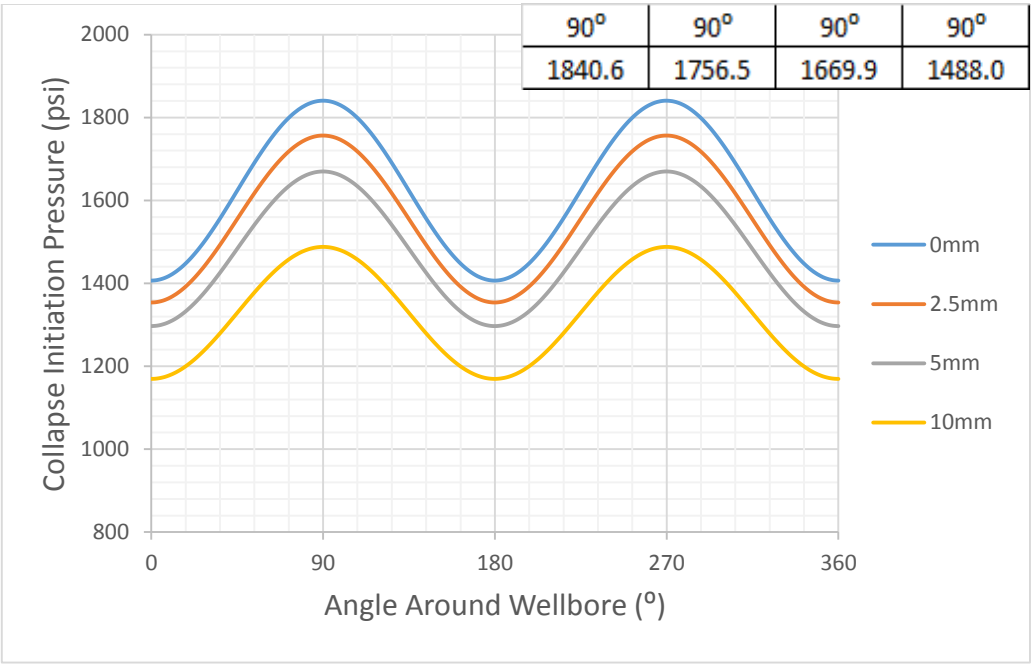

Figure 5.8: Wellbore profile showing effect of mud cake thickness on collapse initiation pressure using Mohr-Coulomb failure criterion.

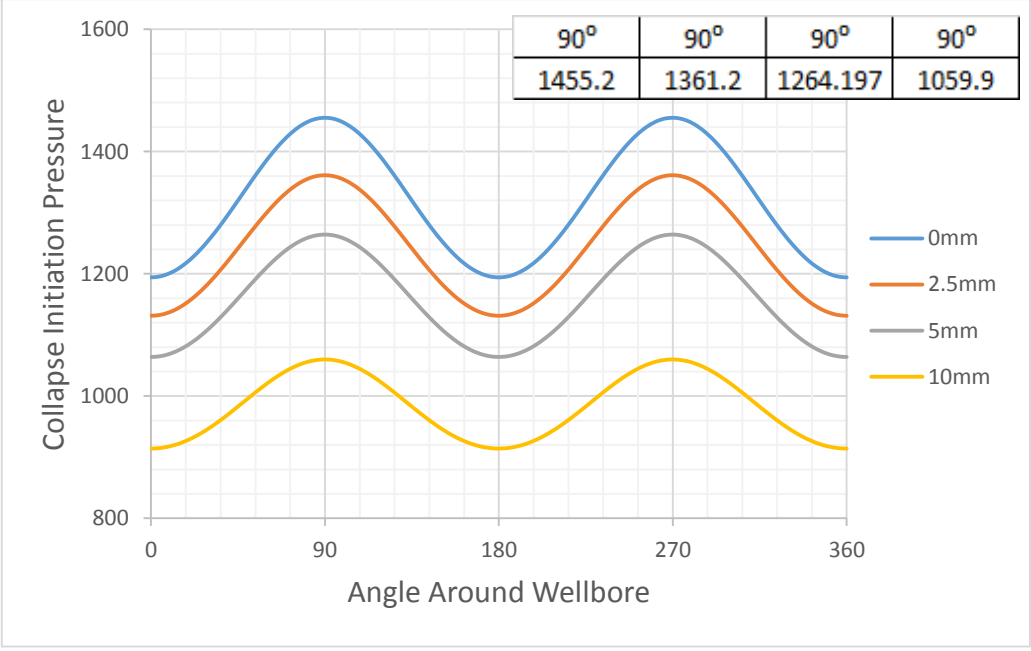

Figure 5.9: Wellbore profile showing effect of mud cake thickness on collapse initiation pressure using Modified Lade failure criterion.

5.4 Effect of Wellbore Size

Three wellbore sizes were simulated to see the effect of the wellbore size on the collapse initiation pressure when mud cake is present. The sizes are 8 in, 12.5 in and 17.25 in wellbores. Figure 5.10 - 5.12 shows this effect for different mud cake thickness using the Mohr-Coulomb failure criterion and Figure 5.13 using the Modified Lade failure criterion. It can be observed that the wellbore strengthening effect of mud cake increases with reducing wellbore sizes and the effect is more pronounced at higher values of mud cake thickness. For this particular case, the collapse initiation pressure at 90^0 was estimated to be 1840.6 psi for the Mohr-Coulomb failure criterion. This implies that when T_{mc} = 2.5 mm, the 8 in, 12.5 in and 17.25 in wellbore got stronger by 133 psi, 84 psi and 61 psi respectively and when T_{mc} = 10 mm, the 8 in, 12.5 in and 17.25 in wellbore got stronger by 573 psi, 353 psi and 251 psi respectively.

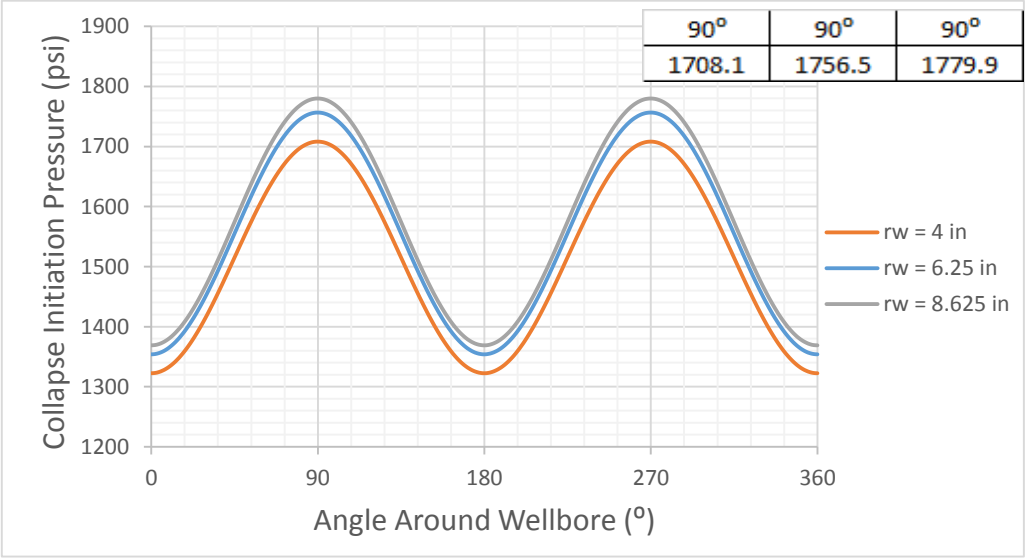

Figure 5.10: Wellbore profile showing effect of wellbore size on collapse initiation pressure using Mohr-Coulomb failure criterion when mud cake thickness is 2.5 mm.

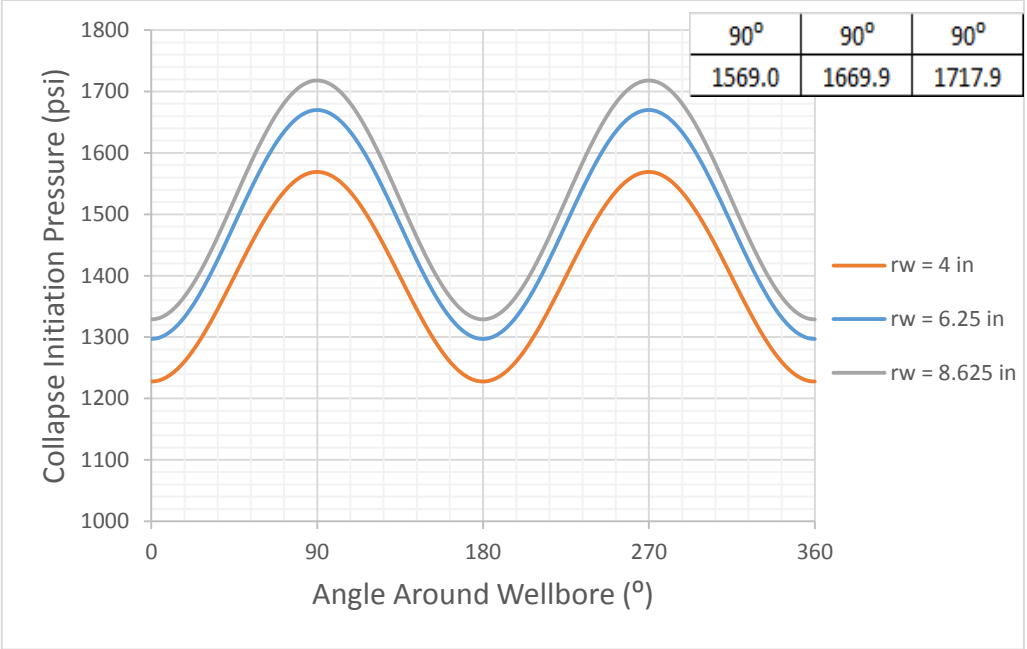

Figure 5.11: Wellbore profile showing effect of wellbore size on collapse initiation pressure using Mohr-Coulomb failure criterion when mud cake thickness is 5 mm.

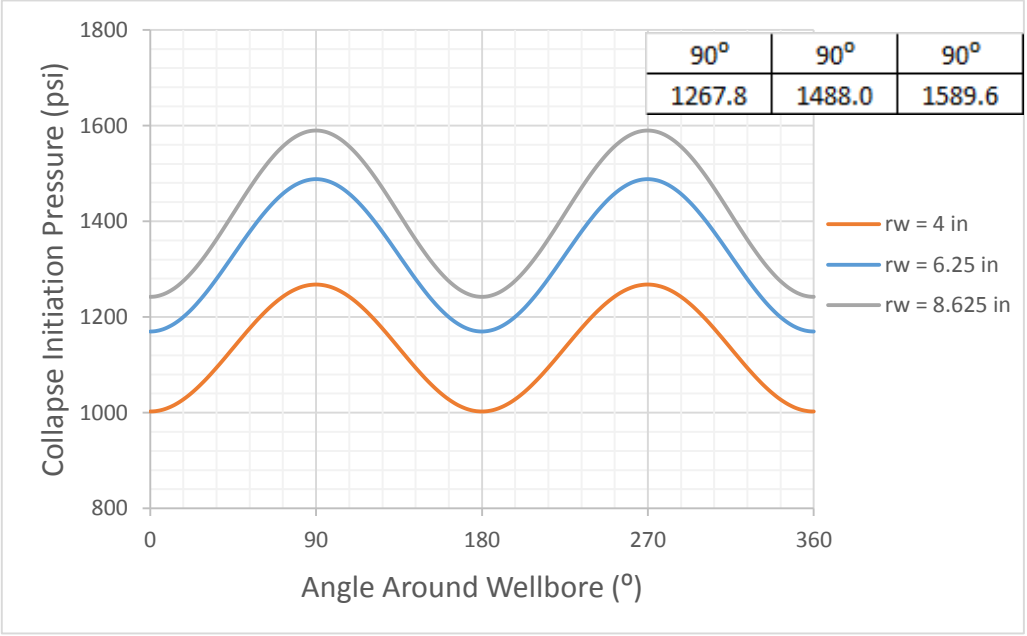

Figure 5.12: Wellbore profile showing effect of wellbore size on collapse initiation pressure using Mohr-Coulomb failure criterion when mud cake thickness is 10 mm.

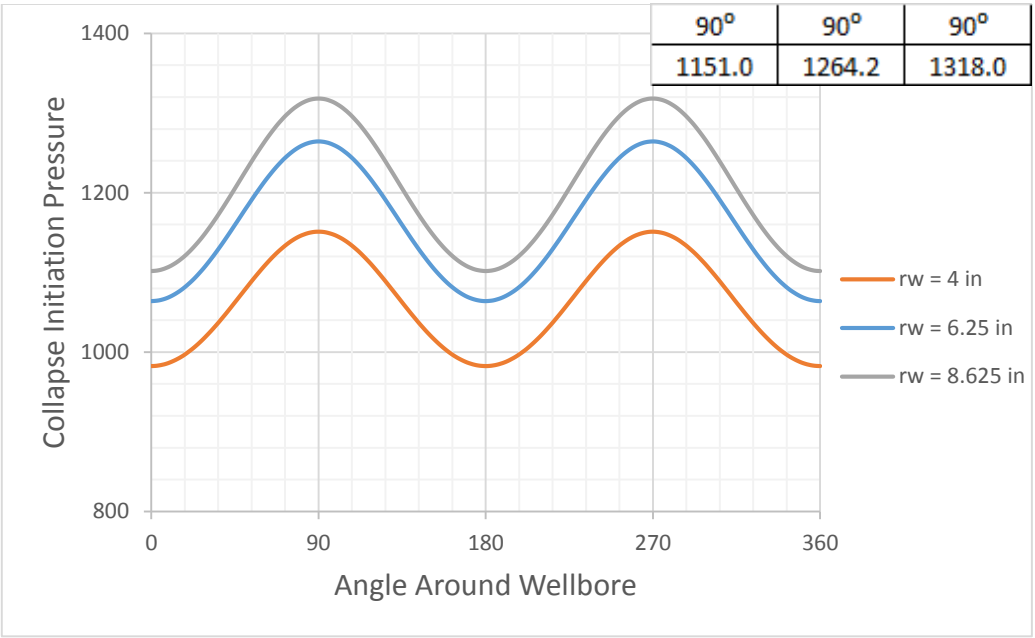

Figure 5.13: Wellbore profile showing effect of wellbore size on collapse initiation pressure using Modified Lade failure criterion when mud cake thickness is 5 mm.

5.5 Effect of Rock Unconfined Compressive Strength

The unconfined compressive strength (UCS) of the rock was varied to see what impact it has on the collapse initiation pressure when mud cake effect is considered. The UCS used for this analysis are 1000 psi, 4000 psi and 7000 psi. Figure 5.14 shows the collapse initiation pressure at point of maximum compression using the Mohr-Coulomb failure criterion and it shows a wellbore strengthening effect as filter cake thickness increases. The wellbore strengthening margin was calculated by subtracting the computed collapse initiation pressure at different values of mud cake thickness from those obtained when mud cake was not considered ($T_{mc} = 0$). This margin gives the error in calculation if mud cake effect was ignored. Figure 5.15 shows the strengthening margin at different mud cake thickness using the Mohr-Coulomb failure criterion and figure 5.16 shows the

same using Modified Lade failure criterion. It can deduced from these charts that, irrespective of failure criteria used, the effect of filter cake on collapse initiation pressure is more significant in harder rocks. For same mud cake thickness, rocks with higher unconfined compressive strength show more strengthening than those with lower UCS.

5.6 Effect of Stress Magnitude/Regime

Two stress scenarios were simulated to see the impact of stress magnitude on this study. The first case had S_{Hmax}, S_{hmin} and S_v as 4000 psi, 3491 psi and 5505 psi respectively, while the second case had S_{Hmax}, S_{hmin} and S_v as 12000 psi, 7215 psi and 5505 psi respectively. The first case represents a normal fault regime, while second case represents a reverse fault regime. In the second case, the difference between horizontal stresses is about 10 times that of the first case. Figure 5.17 shows how much the wellbore is strengthened as a result of mud cake for both cases. It can be seen that the effect was more pronounced in Case 2 than in Case 1. This suggests that more error in collapse initiation pressure calculation will occur in Case 2 if the mud cake effect is ignored compared to Case 1.

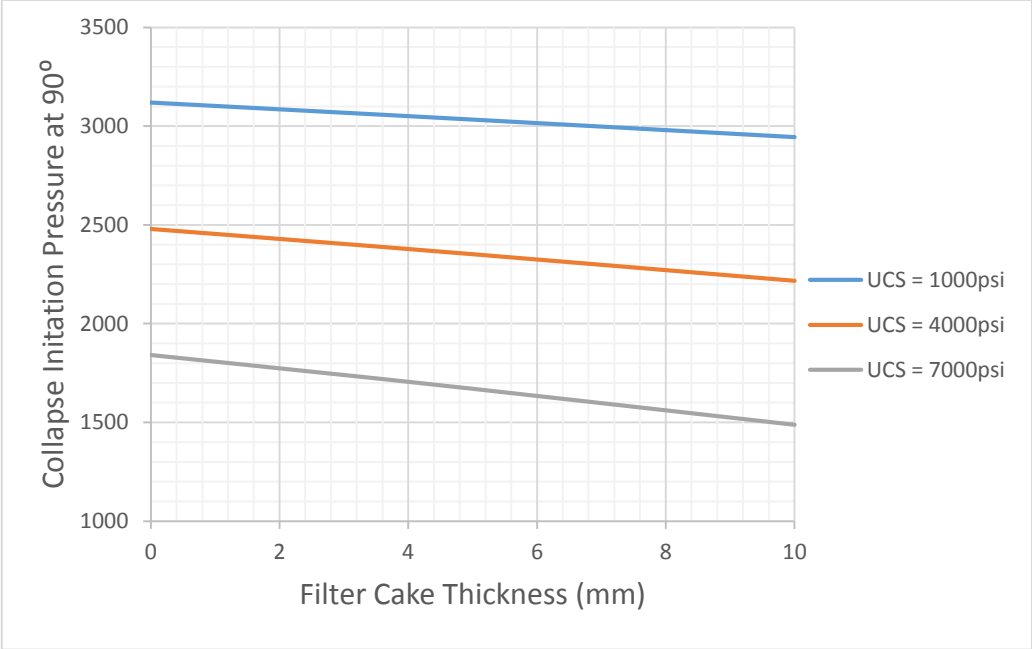

Figure 5.14: Effect of rock unconfined compressive strength on collapse initiation pressure using the Mohr-Coulomb failure criterion.

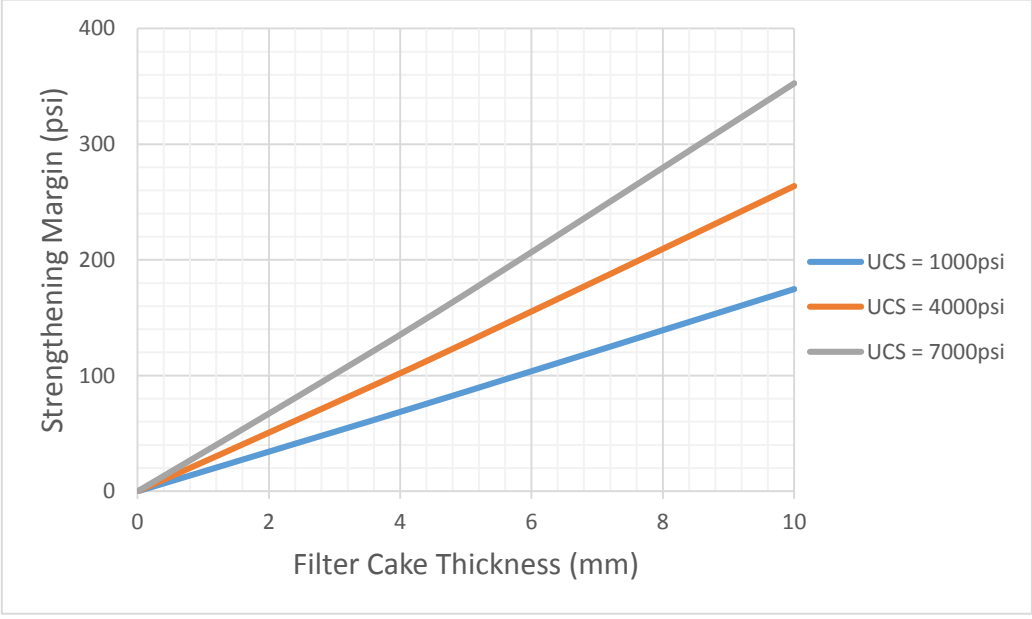

Figure 5.15: Chart showing how much the wellbore is strengthened as a function of the unconfined compressive strength using the Mohr-Coulomb failure criterion.

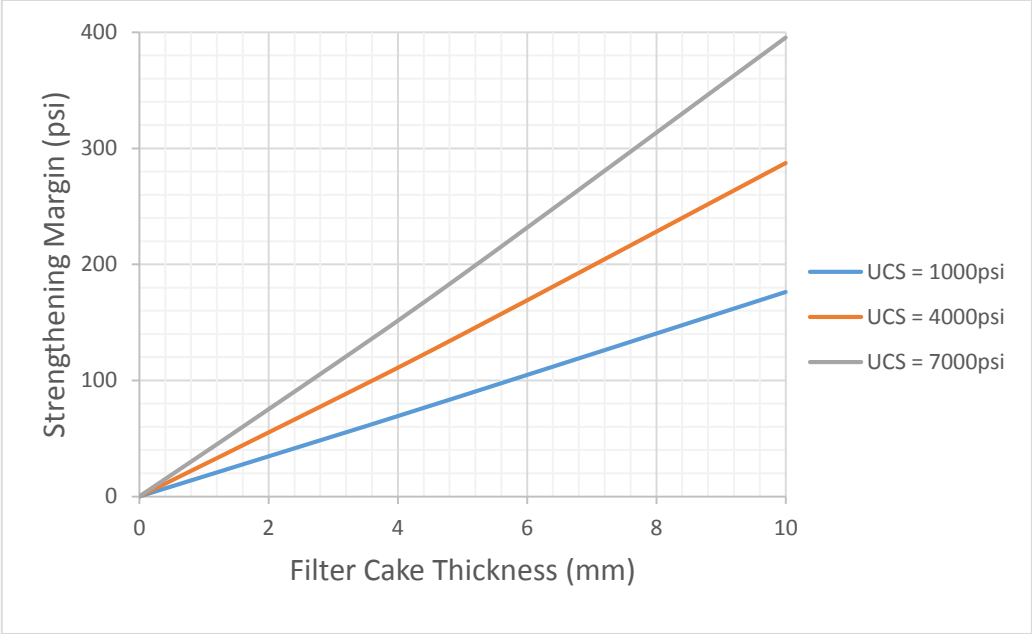

Figure 5.16: Chart showing how much the wellbore is strengthened as a function of the unconfined compressive strength using the Modified Lade failure criterion.

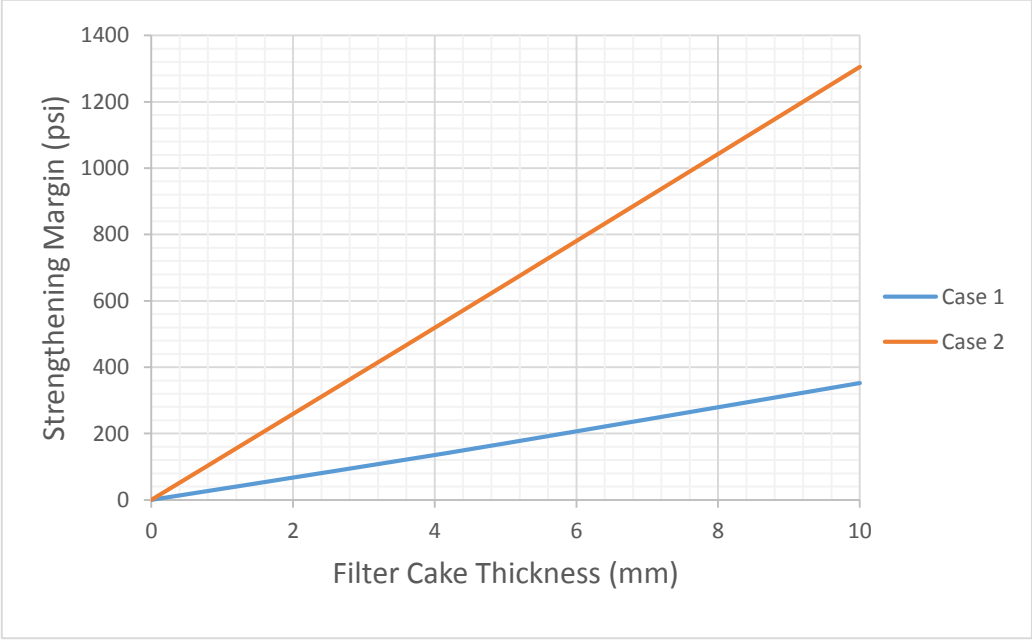

Figure 5.17: Chart showing how much the wellbore is strengthened as a function of the stress magnitude using the Mohr-Coulomb failure criterion.

5.7 Effect of Rock Failure Criterion

All failure criteria show wellbore strengthening effect with mud cake thickness. They only differ in the magnitude of collapse pressure predicted. Table 5.1 shows a summary of collapse initiation pressure at point of maximum compression. It can be observed from the table that the highest collapse initiation pressure was computed using the Inscribed Drucker-Prager failure criterion, while the least collapse initiation pressure was computed using the Circumscribed Drucker-Prager failure criterion at every value of mud cake thickness.

They predicted collapse initiation pressure in the following order from highest to lowest - Inscribed Drucker-Prager, Mohr-Coulomb, Modified lade, then Circumscribed Drucker-Prager. From the result, it can be concluded that Inscribed Drucker-Prager failure criterion predicted the least formation strength and the Circumscribed Drucker-Prager failure criterion predicted the highest formation strength. This is consistent with works by Ewy (1999) and Zoback (2007). Ewy (1999) used 3 failure criterion to estimate collapse initiation pressure and his results showed that Mohr-Coulomb predicted the highest collapse initiation pressure, followed by Modified-Lade, then the Circumscribed Drucker-Prager. Zoback (2007) showed that the Mohr-Coulomb failure criterion yield strength results that fall between those predicted by the Inscribed Drucker-Prager and Circumcised Drucker-Prager failure criteria, with the Inscribed Drucker-Prager predicting the least strength.

	T_{mc} (mm)	0.0	2.5	5.0	10.0
Collapse Initiation Pressure at 90^0 (psi)	IC DP	2495.2	2433.5	2370.3	2239.2
	MC	2480.2	2416.7	2351.7	2216.4
	ML	2224.9	2155.9	2085.2	1937.6
	CS DP	1446.4	1353.1	1256.8	1054.3

Table 5.1: Collapse initiation pressure using different failure criteria when unconfined compressive strength is 4000 psi.
IC DP - Inscribed Drucker-Prager
MC - Mohr-Coulomb
ML - Modified Lade
CS DP - Circumscribed Drucker-Prager
T_{mc} = Mud cake Thickness

CHAPTER VI

EFFECT OF TEMPERATURE ON COLLAPSE INITIATION PRESSURE WITH MUD CAKE EFFECT

The effect of temperature was studied when mud cake is present. We would expect mud cake to form in permeable formations like sandstone and not shale. Young's Modulus of sandstone ranges from 0.7×10^6 psi to 12.2×10^6 psi (Watson et al. 2003). Coefficient of linear thermal expansion of rocks is strongly dependent on the quantity of silica present in the rock, with coefficient of linear thermal expansion varying from $\sim 10^{-6}\ ^0\mathrm{C}^{-1}$, when silica content is 0%, to $\sim 10^{-5}\ ^0\mathrm{C}^{-1}$, when silica content is 100%; sandstone have coefficient of linear thermal close to $10^{-6}\ ^0\mathrm{C}^{-1}$ (Zoback 2007). For these reasons, Young's Modulus of 6×10^6 psi and coefficient of linear thermal expansion of $9 \times 10^{-6}\ ^0\mathrm{C}^{-1}$ was used in this part of the study.

Generally, the wellbore gets strengthened (lower collapse initiation pressure) due to cooling and gets weakened (higher collapse initiation pressure) due to wellbore heating (Figure 6.1 and Figure 6.2). This is consistent with past works such as Chen and Ewy (2005), Guenot and Santarelli (1989), and Tran (2010).

The effect of mud cake compressibility on this study was first investigated. Like in the effect of mud cake alone, the mud cake compressibility did not show any impact on the effect of temperature when mud cake is present (Figure 6.3 and Figure 6.4). Unlike in the effect of mud cake, where the rock unconfined compressive strength increases the rock strengthening effect of mud cake, the strengthening/weakening effect is constant at a fixed

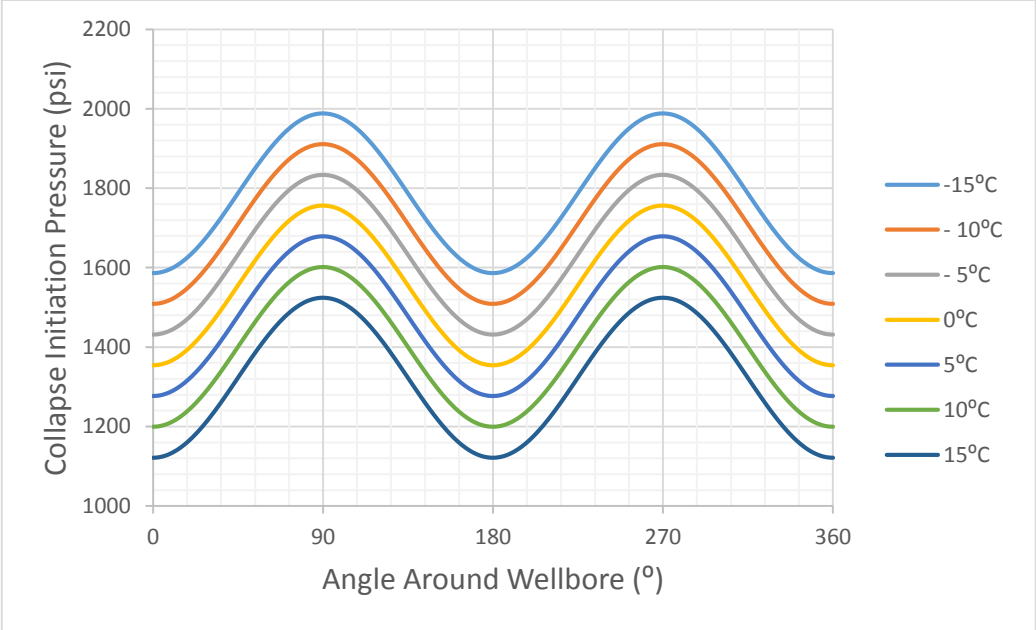

Figure 6.1: Wellbore profile showing effect of temperature on collapse initiation pressure using Mohr-Coulomb failure criterion when mud cake thickness is 2.5 mm and unconfined compressive strength of 7000 psi.

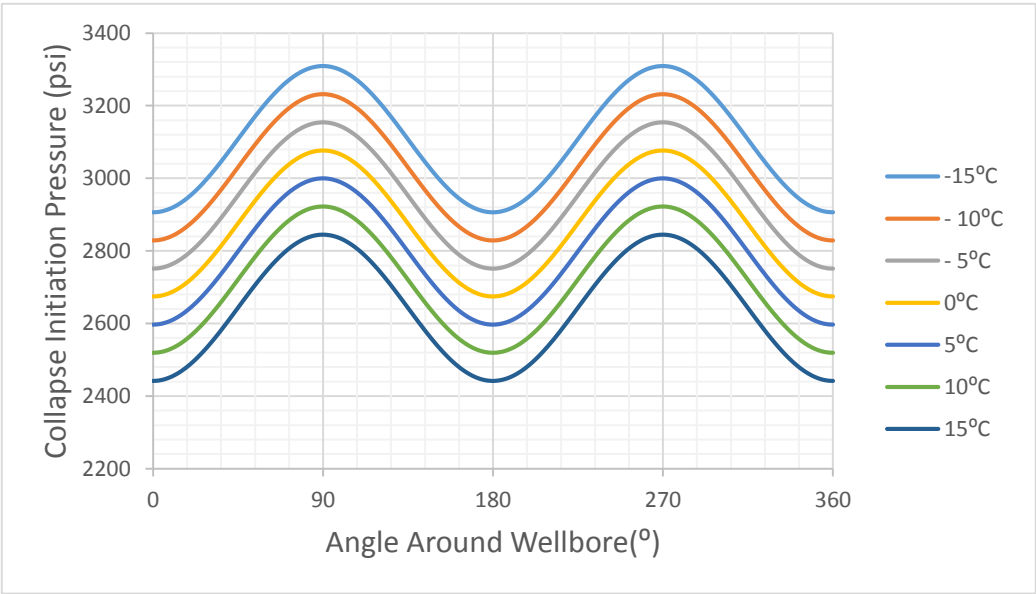

Figure 6.2: Wellbore profile showing effect of temperature on collapse initiation pressure using Mohr-Coulomb failure criterion when mud cake thickness is 2.5 mm and unconfined compressive strength of 1000 psi.

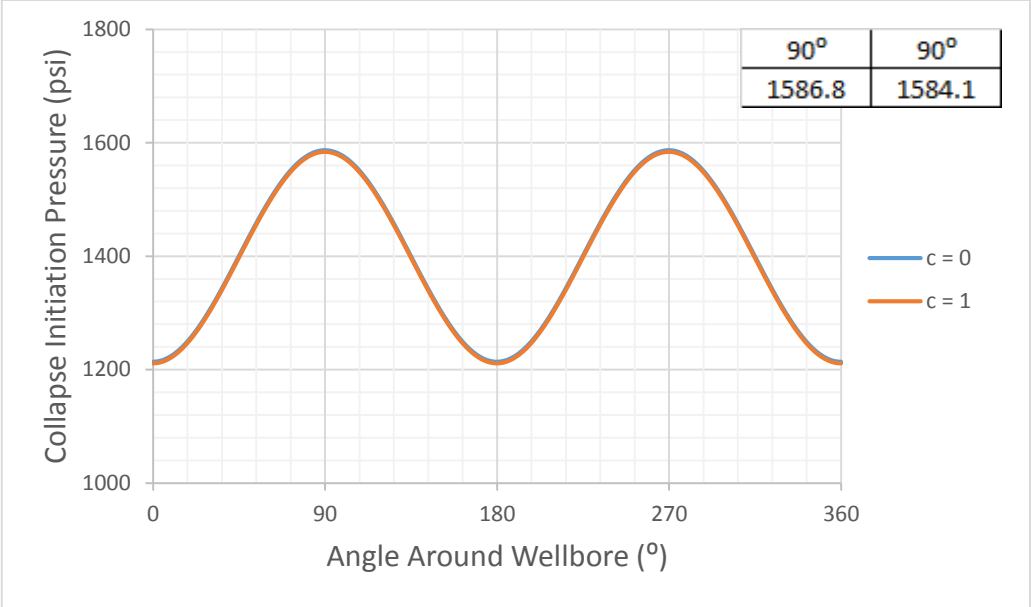

Figure 6.3: Wellbore profile showing effect of compressibility exponent on collapse initiation pressure using Mohr-Coulomb failure criterion when mud cake thickness is 5 mm with 5 ^{0}C wellbore cooling.

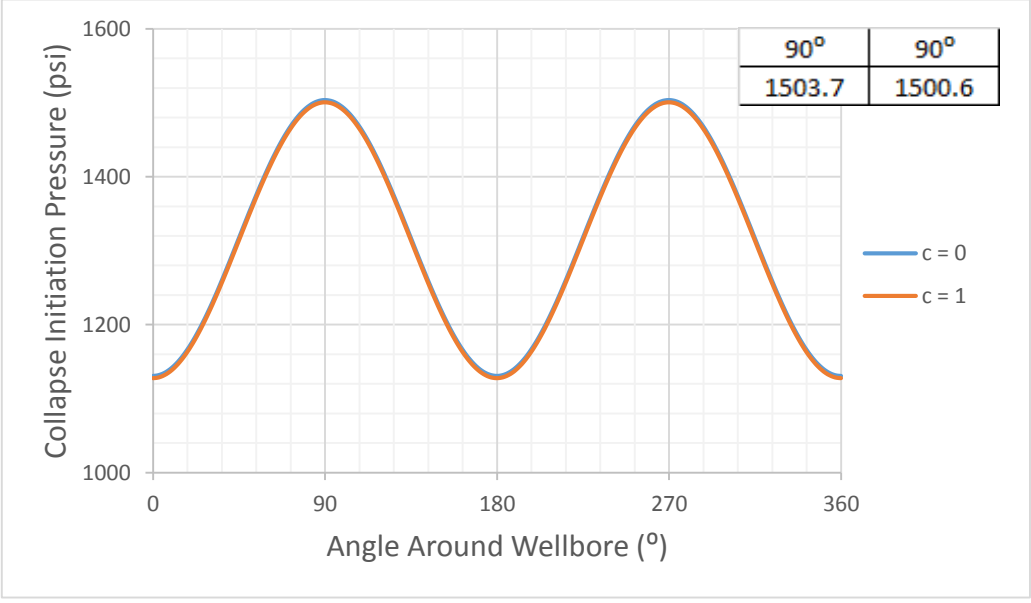

Figure 6.4: Wellbore profile showing effect of compressibility exponent on collapse initiation pressure using Mohr-Coulomb failure criterion when mud cake thickness is 5 mm with 10 ^{0}C wellbore cooling.

mud cake thickness for different rock unconfined compressive strength. The wellbore strengthening margin was calculated by subtracting the computed collapse initiation pressure at different values of wellbore cooling or heating from those obtained when temperature effect was not considered ($\Delta T = 0$) at different values of mud cake thickness. Figures 6.5 and 6.6 shows the wellbore strengthening margin plotted against mud cake thickness at different unconfined compressive strength. The plots show that the UCS did not have any effect on the wellbore strengthening margin but this margin increases as mud cake thickness increases. This implies that the presence of mud cake amplifies the effect of temperature, with increasing effect as mud cake thickness increases.

Tables 6.1, 6.2 and 6.3 shows collapse initiation pressure at point of maximum compression computed for wellbore cooling and heating at different mud cake thicknesses and unconfined compressive strengths. It should be noted that positive ΔT is wellbore cooling and negative ΔT is wellbore heating. It can be observed from these tables that the collapse initiation pressure decreases from left to right as the difference between the temperature of wellbore fluid and formation (ΔT) changes from 0 ^{0}C to 15 ^{0}C and increases from right to left as ΔT changes from 0 ^{0}C to -15 ^{0}C. Also, the collapse initiation pressure decreases as the mud cake thickness increases from 0 mm to 10 mm. This implies that both wellbore cooling and mud cake effect strengthen the formation, while wellbore heating weakens the formation.

Finally, when UCS was 1000 psi, the effect of wellbore cooling was higher than that of mud cake. As the UCS increases from 1000 psi to 7000 psi, this trend reverses with the mud cake effect higher than that of wellbore cooling.

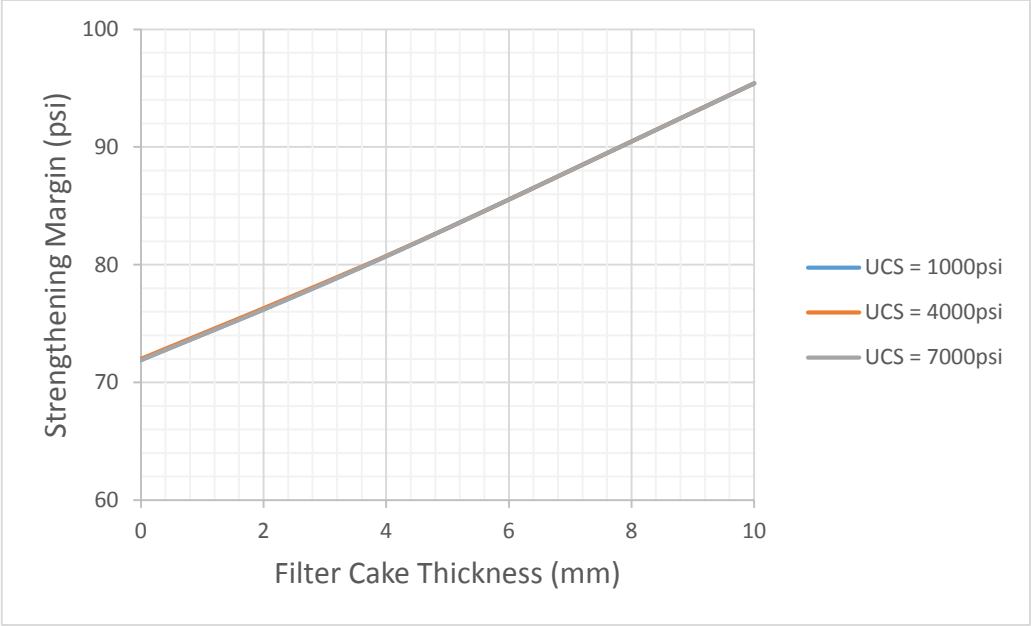

Figure 6.5: Chart showing how much the wellbore is strengthened as a function of the unconfined compressive strength using the Mohr-Coulomb failure criterion with 5 ^{0}C wellbore cooling.

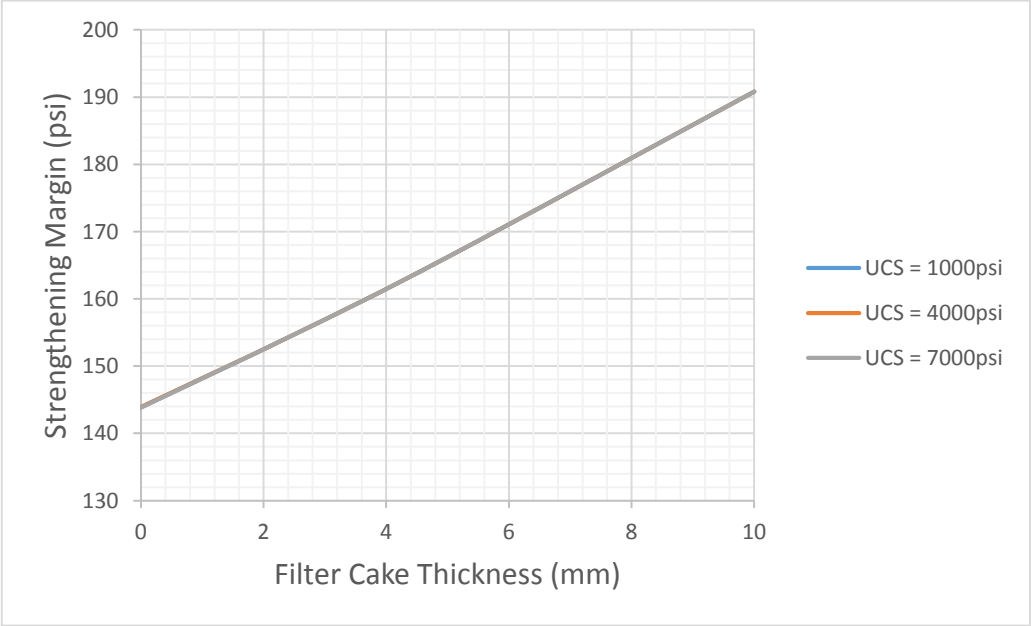

Figure 6.6: Chart showing how much the wellbore is strengthened as a function of the unconfined compressive strength using the Mohr-Coulomb failure criterion with 10 ^{0}C wellbore cooling.

ΔT	-15^{0}C	- 10^{0}C	- 5^{0}C	0^{0}C	5^{0}C	10^{0}C	15^{0}C
T_{mc} (mm)	Collapse Initiation Pressure at 90^0 (psi)						
0.0	3335.5	3263.5	3191.6	3119.7	3047.8	2975.8	2903.9
2.5	3309.0	3231.6	3154.2	3076.8	2999.5	2922.1	2844.7
5.0	3282.7	3199.6	3116.5	3033.5	2950.4	2867.3	2784.2
10.0	3230.9	3135.5	3040.1	2944.8	2849.4	2754.0	2658.6

Table 6.1: Summary table showing effect of temperature on collapse initiation pressure at different mud cake thicknesses when unconfined compressive strength is 1000 psi using Mohr-Coulomb failure criterion.

ΔT	-15^{0}C	- 10^{0}C	- 5^{0}C	0^{0}C	5^{0}C	10^{0}C	15^{0}C
T_{mc} (mm)	Collapse Initiation Pressure at 90^0 (psi)						
0.0	2695.9	2624.0	2552.1	2480.2	2408.2	2336.3	2264.4
2.5	2648.8	2571.4	2494.1	2416.7	2339.3	2262.0	2184.6
5.0	2600.9	2517.8	2434.7	2351.7	2268.6	2185.5	2102.4
10.0	2502.5	2407.1	2311.7	2216.4	2121.0	2025.6	1930.2

Table 6.2: Summary table showing effect of temperature on collapse initiation pressure at different mud cake thicknesses when unconfined compressive strength is 4000 psi using Mohr-Coulomb failure criterion.

ΔT	-15^{0}C	- 10^{0}C	- 5^{0}C	0^{0}C	5^{0}C	10^{0}C	15^{0}C
T_{mc}(mm)	Collapse Initiation Pressure at 90^0						
0mm	2056.4	1984.5	1912.6	1840.6	1768.7	1696.8	1624.9
2.5mm	1988.6	1911.3	1833.9	1756.5	1679.2	1601.8	1524.4
5mm	1919.1	1836.0	1752.9	1669.9	1586.8	1503.7	1420.6
10mm	1774.1	1678.7	1583.3	1488.0	1392.6	1297.2	1201.8

Table 6.3: Summary table showing effect of temperature on collapse initiation pressure at different mud cake thicknesses when unconfined compressive strength is 7000 psi using Mohr-Coulomb failure criterion.

CHAPTER VII

CONCLUSIONS AND FUTURE WORKS

7.1 Conclusions

1. Ignoring the effect of temperature or mud cake can lead to erroneous collapse initiation pressure estimation.
2. Sensitivity analysis performed on the effect of mud cake on collapse initiation pressure showed that the mud cake compressibility had negligible effect on the analysis as the collapse initiation pressure decreases with increasing mud cake thickness.
3. Collapse initiation pressure when mud cake is present depends on wellbore size, with the wellbore getting stronger as the wellbore size reduces.
4. Effect of mud cake on collapse initiation pressure is more pronounced in rocks with higher unconfined compressive strength.
5. Effect of mud cake might be negligible at low stress magnitudes but gets more significant as the stress level increases.
6. Effect of temperature coupled with mud cake effect showed that both mud cake and wellbore cooling tends to strengthen the wellbore, while wellbore heating reduces the strength of the formation.
7. Mud cake compressibility have a minor impact on effect of temperature coupled with mud cake effect, hence, an incompressible mud cake can be assumed and still get accurate results.

8. Presence of mud cake tends to amplify the effect of temperature, with increasing effect as the mud cake thickness increases.

7.2 Future Works

It should be noted that this work used a static approach in it analysis. It does lend itself to more work in future, as there are still several questions that could be posed and more analysis that could be done.

A more rigorous and robust approach should consider the following:

1. A technique for accurate determination of mud cake thickness and properties
2. Reduction of mud cake thickness as a result of the erosion of mud cake as wellbore fluid flow in the annulus between wall of formation and drill strings assembly.
3. Increase in mud cake thickness as a result of deposition of more mud cake.

REFERENCES

1. Aadnoy, B., Belayneh, M., Arriado Jorquera, M., & Flateboe, R., 2008, "Design of Well Barriers to Combat Circulation Losses", SPE Journal of Drilling & Completion, 23(3), 2008, 295–300. doi:10.2118/105449-PA.
2. Aadnøy, B., & Looyeh, R., 2011, "Petroleum Rock Mechanics: Drilling Operations and Well Design", Burlington: [electronic resource] Elsevier Science, ISBN: 9780123855473.
3. Abdulhadi, N. O., 2009, "An Experimental Investigation into the Stress-Dependent Mechanical Behavior of Cohesive Soil with Application to Wellbore Instability", PhD Dissertation. Department of Civil & Environmental Engineering, MIT, Cambridge, MA.
4. Abdulhadi, N. O., Germaine, J. T., & Whittle, A. J., 2011, "Experimental Study of Wellbore Instability in Clays". Journal of Geotechnical and Geoenvironmental Engineering, (August), 766–776. doi:10.1061/(ASCE)GT.1943-5606.0000495.
5. Abousleiman, Y.N., Nguyen, V., Hemphill, T., & Kanj, M.Y, 2007, "Time-Dependent Wellbore Strengthening in Chemically Active or Less Active Rock Formations". AADE-07-NTCE-67 presented at the 2007 AADE National Technical Conference and Exhibition, Houston, 10–12 April.
6. Adams, N. J., & Kuhlman, L. G., 1991, "Shallow Gas Blowout Kill Operations", SPE 21455 presented at the SPE Middle East Oil Show held in Bahrain, 16-19 November 1991.

7. Akl, S. A., 2011, “Wellbore Instability Mechanisms in Clays. PhD Dissertation”, Department of Civil & Environmental Engineering, MIT, Cambridge, MA.
8. Bejarbaneh, B. Y., Armaghani, D. J., & Amin, M., 2015, “Strength Characterisation of Shale Using Mohr – Coulomb and Hoek – Brown criteria”, Elsevier Measurement 63, 269–281. doi:10.1016/j.measurement.2014.12.029.
9. Bureau of Safety and Environmental Enforcement (BSEE) website: http://www.bsee.gov/Regulations-and-Guidance/Notices-to-Lessees- and-Operators.aspx
10. Bradley, W. B., 1979, “Failure of Inclined Boreholes”. Journal of Energy Resources Technology, 101(December 1979), 232. doi:10.1115/1.3446925.
11. Calçada, L. A., Scheid, C. M., Calabrez, N. D., Rural, F., & Janeiro, R. De, 2014, “A Simplified Methodology for Dynamic Drilling Fluid Filtration Estimation Considering Mudcake Compressibility”. SPE 168208.
12. Cheatham, J. C., 1984, “Wellbore Stability”, Journal of Petroleum Technology, (June), 889–896. Retrieved from https://www.onepetro.org/journal-paper/SPE-13340-PA.
13. Chen, G., & Ewy, R.T., 2005, “Thermoporoelastic Effect on Wellbore Stability”, SPE 89039, June 2005 SPE Journal.
14. Chi, A. I., Yuwei, L. I., & Yu, L. I. U, 2013, “The Effects of Pore Pressure and Temperature Difference Variation on Borehole Stability”, Advances in Petroleum Exploration and Development 6(1), 22–26. doi:10.3968/j.aped.1925543820130601.1546.

15. Choi, S.K. & Tan, C.P., 1998, "Modeling Effects of Drilling-Fluid Temperature on Wellbore Stability", SPE 47304, SPE/ISRM Rock Mechanics in Petroleum Engineering, 8-10 July 1998, Trondheim, Norway.
16. Dananberger, E.P, 1993, "Outer Continental Shelf Drilling Blowouts, 1971-1991", paper OTC 7248, presented at the 25th Ann. OTC, Houston, TX, USA, 3-6 May 1993.
17. Dewan, J., & Chenevert, M., 2001, "A Model for Filtration of Water-Base Mud during Drilling: Determination of Mudcake Parameters", Petrophysics, 42(3), 237–250. Retrieved from https://www.onepetro.org/journal-paper/SPWLA-2001-v42n3a4.
18. Ewy, R. T., 1999, "Wellbore-Stability Predictions by Use of a Modified Lade Criterion", SPE Drilling & Completion, 14(2), 85–91. doi:10.2118/56862-PA.
19. Fett, J., Martin, F., Dardeau, C., Rignol, J., Benaissa, S., Adachi, J., & Pastor, J., 2009, "Case History: Successful Wellbore Strengthening Approach in a Depleted and Highly Unconsolidated Sand in Deepwater Gulf of Mexico", SPE Drilling & Completion, 25(4). doi:10.2118/119748-PA.
20. Fjaer, E., Holt, R.M., and Horsrud, P., 2008, "Petroleum Related Rock Mechanics", Second Edition. Amsterdam; London: Elsevier, 2008. ISBN: 9780444502605.
21. Gabrielsen, G. K., Stenebråten, J. F., Nes, O.-M., Holt, R. M., & Horsrud, P., 2010, "Use of Modified Hollow Cylinder Test in Laboratory for Simulation of Downhole Drilling Condition in Shale", SPE 131356.
22. Gabrielsen, G. K., Stenebråten, J. F., Nes, O.-M., Horsrud, P., & Saasen, A., 2011, "Improved Understanding of the Effects from Drill String RPM in Shale through Dedicated Hollow Cylinder Laboratory Tests", Rock Mechanics.

23. Guenot, A., & Santarelli, F. J., 1989, "Influence of Mud Temperature on Deep Borehole Behavior", Rock at Great Depth, Maury & Fourmaintraux, Rotterdam. ISBN 90 6191 975 4.
24. Grøttheim, O., 2005, "Development and Assessment of Electronic Manual for Well Control and Blowout Containment Development and Assessment of Electronic Manual", MS Thesis. Petroleum Engineering Department, Texas A&M University, College Station, Texas.
25. Islam, M. A., & Skalle, P., 2011, "Calibration of Rock Strength and Yielding By Using Hollow Cylinder Experimental Data". American Rock Mechanics Association.
26. Jourine, S., Schubert, J.J, & Valkó, P.P., 2004, "Saturated Poroelastic Hollow Cylinder Subjected to Non-Stationary Boundary Pressure – Model and Laboratory Test", Paper 541, presented at the 2004 North American Rock Mechanics Symposium (Gulfrocks), Houston, TX June 5-10 2004.
27. Kang, Y., Yu, M., Miska, S., & Takach, N, 2009, "Wellbore Stability: A Critical Review and Introduction to DEM". SPE Annual Technical October, 4–7. Retrieved from SPE-124669-MS
28. Labenski, F., Reid, P., & Santos, H., 2003, "Drilling Fluids Approaches for Control of Wellbore Instability in Fractured Formations", SPE / IADC 85304.
29. Lal, M., 1999, "Shale Stability : Drilling Fluid Interaction and Shale Strength", SPE 54356 Latin American and Caribbean Petroleum Engineering Conference held in Caracas, Venezuela, 21–23 April 1999.

30. Li, G., & Bai, M., 2012, “Parametric Sensitivity Investigation: Analysis of Wellbore Stability”, Harmonising Rock Engineering and the Environment – Qian & Zhou (eds) © 2012 Taylor & Francis Group, London, ISBN 978-0-415-80444-8, 2091–2096.
31. Li, X., Cui, L., & Roegiers, J.C., 1998, “Thermoporoelastic Analyses of Inclined Boreholes”, SPE 47296, SPE/ISRM Rock Mechanics in Petroleum Engineering, 8-10 July 1998.
32. Marsden, R., Dennis, W., & Wu, B., 1996, “Deformation and Failure of Thick-Walled Hollow Cylinders of Mudrock: A Study of Wellbore Instability in Weak Rock Deformation”, et rupture de cylindres creux a paroi epaisse en roches argileuses.
33. McLean, M., & Addis, M., 1990, “Wellbore Stability Analysis: A Review of Current Methods of Analysis and their Field Application”, SPE/IADC Drilling Conference.
34. McLean, M., & Addis, M., 1990, “Wellbore Stability Analysis: The Effect of Strength Criteria on Mud Weight Recommendations”, SPE/IADC Drilling Conference.
35. Mostafavi, V., Hareland, G., Aadnoy, B. S., & Kustamsi, A., 2010, “Modeling of Fracture and Collapse Initiation Gradients in Presence of Mud Cake”, Rock Mechanics in Civil and Environmental Engineering – Zhao, Labiouse, Dudt & Mathier (eds), ISBN 978-0-415-58654-2, 725–728.
36. Nes, O.-M., Stenebråten, J., & Fjær, E., 2015, “Time Dependent Borehole Stability: Effect of Static vs. Dynamic Mud Weight”, Society of Petroleum Engineers. SPE/IADC Drilling Conference and Exhibition, doi:10.2118/173048-MS.

37. Nesheli, B.A., 2006, “Rock Mechanics Aspects of Blowout Rock Mechanics Aspects of Blowout”, MS Thesis. Petroleum Engineering Department, Texas A&M University, College Station, Texas.
38. Nesheli, B.A. & Schubert, J.J., 2006, ”Effect of Water Depth on Bridging Tendencies in Ultra-Deepwater Blowouts in Gulf of Mexico”, SPE 103139, presented at the 2006 SPE ATCE, San Antonio, TX, USA 24-27 September 2006.
39. Pašić, B., 2007, “Wellbore Instability: Causes and Consequences”, Rudarsko-Geološko-Naftni zbornik, Vol 19, Str 87-98, Retrieved from http://hrcak.srce.hr/index.php?show=clanak&id_clanak_jezik=30197.
40. Salisbury, D., Ramos, G., & Wilton, B., 1991, “Wellbore Instability of Shales Using a Downhole Simulation Test Cell”. Rock Mechanics as a Multidisciplinary Science, Roegiers (ed), ISBN906191.
41. Skalle, P., Jinjun, H., Podio, A.L., 1999, “Killing Methods and Consequences of 1120 Gulf Coast Blowouts during 1960-1996”, SPE 53974 presented at the 1999 SPE Latin America and Caribbean Petroleum Engineering conference held in Caracas, Venezuela, 23-23 April 1999.
42. Shewalla, M. 2007, “Evaluation of Shear Strength Parameters of Shale and Siltstone”, MS Thesis, (December). The Department of Civil and Environmental Engineering, Louisiana State University, Louisiana.
43. Smith, L.M., 2012, “A Review of Offshore Blowouts and Spills to Determine Desirable Capabilities of a Subsea Capping Stack”, MS Thesis, May 2012. The Craft

and Hawkins Department of Petroleum Engineering, Louisiana State University, Louisiana.

44. Tran, D., 2010, "Thermal Effects in Borehole Stability", PhD Dissertation, University of Oklahoma. Norman, Oklahoma.
45. Watson, D., Brittenham, T., & Moore, P., 2003, "Advanced Well Control", SPE Textbook Series Vol. 10, Society of Petroleum Engineers (SPE), Richardson, Texas. ISBN 1-55563-101-0
46. Wilson, S., 2012, "A Wellbore Stability Approach for Self-Killing Blowout Assessment", SPE 156330 presented at the SPE Deepwater Drilling and Completions Conference held in Galveston, Texas, USA, 20–21 June 2012.
47. Wilson, S.M., Nagoo, A.S., & Sharma, M.M., 2013, "Analysis of Potential Bridging Scenarios during Blowout Event". SPE/IADC 163438 presented at the SPE/IADC Drilling Conference and Exhibition held in Amsterdam, the Netherlands, 5–7 March 2013.
48. Wu, B., Tan, C., & Chen, X., 2000, "Plane Strain Effect on Strength and Deformation of Hollow Cylinders of Shale", Pacific Rocks 2000, Girard, Liebman, Breeds & Doe (eds). ISBN 90 5809 155 4
49. Xu, G., 2007, "Wellbore Stability in Geomechanics", PhD Dissertation. The University of Nottingham. Retrieved from http://etheses.nottingham.ac.uk/1475/
50. Zoback, MD., 2007, "Reservoir Geomechanics", Cambridge: Cambridge University Press, ISBN: 0521770696.